The Sar1 GTPase Coordinates Biosynthetic Cargo Selection with Endoplasmic Reticulum Export Site Assembly✪

Meir Aridor,* Kenneth N. Fish,*‡ Sergei Bannykh,* Jacques Weissman,* Theresa H. Roberts,§ Jennifer Lippincott-Schwartz,§ and William E. Balch*‖

*Department of Cell and Molecular Biology, and ‖The Institute of Childhood and Neglected Diseases, The Scripps Research Institute, La Jolla, California 92037; ‡The Harold L. Dorris Neurological Research Center, and §Cell Biology and Metabolism Branch, National Institute of Child Health and Human Development, National Institutes of Health, Bethesda, Maryland 20892

Abstract. Cargo selection and export from the endoplasmic reticulum is mediated by the COPII coat machinery that includes the small GTPase Sar1 and the Sec23/24 and Sec13/31 complexes. We have analyzed the sequential events regulated by purified Sar1 and COPII coat complexes during synchronized export of cargo from the ER in vitro. We find that activation of Sar1 alone, in the absence of other cytosolic components, leads to the formation of ER-derived tubular domains that resemble ER transitional elements that initiate cargo selection. These Sar1-generated tubular domains were shown to be transient, functional intermediates in ER to Golgi transport in vitro. By following cargo export in live cells, we show that ER export in vivo is also characterized by the formation of dynamic tubular structures. Our results demonstrate an unanticipated and novel role for Sar1 in linking cargo selection with ER morphogenesis through the generation of transitional tubular ER export sites.

Key words: Sar1 • COPII • endoplasmic reticulum • vesicle • cargo export

Introduction

The endoplasmic reticulum is the first compartment of the secretory pathway. The transport activity of the ER was first described morphologically by the pioneering work of Palade (1975). Ribosome-bound specialized regions in the compartment are devoted to protein synthesis, whereas smooth extended tubular domains, the transitional elements, participate in vesicle-mediated export of cargo. These morphological specializations led to the suggestion that there may be a dynamic domain organization to the otherwise continuous reticulum.

The biochemical basis for ER export is beginning to be unraveled. It is now recognized that cytosolic coat proteins of the COPII family are recruited to specialized ER export sites that mediate vesicle formation (Aridor et al., 1995; Bannykh et al., 1996; Scales et al., 1997; Martinez-Menarguez et al., 1999). Cargo, including newly synthesized proteins that are delivered to distinct cellular and extracellular destinations (biosynthetic cargo) and recycling proteins that comprise the membrane-bound transport machinery, is sorted into these ER-derived COPII-coated vesicles (Barlowe et al., 1994; Rexach et al., 1994; Aridor and Balch, 1996; Bannykh et al., 1996; Aridor et al., 1998). The COPII coat machinery includes the soluble GTPase Sar1 and two cytosolic protein complexes, Sec23/24 and Sec13/31. These components are sufficient to direct vesicle budding from ER membranes (Barlowe et al., 1994; Matsuoka et al., 1998). Cargo sorting is initiated by assembly of detergent-soluble prebudding complexes that contain cargo and coat subunits. The complex is formed in response to the activation of Sar1 and the subsequent recruitment of the Sec23/24 complex (Aridor et al., 1998; Kuehn et al., 1998). Completion of budding and vesicle fission requires the recruitment of the Sec13/31 protein complex. In mammalian cells, the cargo exiting the ER is contained within vesicular tubular clusters (VTCs)[1] (Balch et al., 1994). These intermediates initiate the process of segregation of retrograde from anterograde cargo through the activity of a second coat machinery, the COPI complex (Aridor et al., 1995). Subsequently, through dynein motor activity, mature

✪The online version of this article contains supplemental material.

Address correspondence to William E. Balch, Department of Cell and Molecular Biology, The Scripps Research Institute, 10550 N. Torrey Pines Road, La Jolla, CA 92037. Tel.: 858-784-2310. Fax: 858-784-9126. E-mail: webalch@scripps.edu

Dr. Aridor's current address is Department of Cell Biology and Physiology, University of Pittsburgh School of Medicine, 3500 Terrace Street, BST South 362, Pittsburgh, PA 15251.

[1]*Abbreviations used in this paper:* BIP, immunoglobulin binding protein; DIC, differential interference contrast; DTSSP, 3′-dithiobissulfosuccimidylpropionate; GFP, green fluorescent protein; GST, glutathione-S-transferase; Man II, 1,2-mannosidase II; MT, microtubule; NRK, normal rat kidney; VTC, vesicular tubular cluster.

VTCs move along microtubules (MTs) to deliver cargo to the perinuclear Golgi complex (Presley et al., 1997).

The mechanism by which the sequential assembly of components of the COPII coat machinery mobilize biosynthetic cargo for transport to downstream compartments remains to be determined. We have, therefore, analyzed the initial steps of cargo selection in the ER using a synchronized ER export assay. We show morphologically using indirect immunofluorescence that the Sar1 GTPase alone can initiate membrane cargo selection before recruitment and assembly of the other COPII cytosolic coat complexes. Activation of Sar1 couples cargo sorting with the formation of striking tubular domains emanating from the ER. These tubules are rapidly consumed upon addition of the COPII coat complexes Sec23/24 and Sec13/31 to form VTCs that deliver concentrated cargo to the Golgi. Our results suggest an unanticipated role for the Sar1 GTPase in ER morphogenesis leading to the formation of specialized export domains. These data provide a molecular link between the biochemical events of ER export involved in cargo selection and the morphological steps directing the delivery of cargo to post-ER compartments.

Materials and Methods

Materials

Antibodies to glutathione-S-transferase (GST) protein, mammalian Sar1, mammalian Sec23, mammalian Sec22, and VSV-G were prepared as described (Plutner et al., 1992; Kuge et al., 1994; Aridor et al., 1995; Rowe et al., 1996). Antibody to 1,2-mannosidase II (Man II) was kindly provided by Dr. M Farquhar (University of California at San Diego, San Diego, CA). Antibody to immunoglobulin binding protein (BIP) was purchased from StressGen Biotechnologies. Recombinant wild-type Sar1, Sar1[T39N], and Sar1[H79G] mutants were expressed and purified as described (Kuge et al., 1994; Aridor et al., 1995; Rowe and Balch, 1995; Rowe et al., 1996). Recombinant myristoylated ARF1[Q71L] was expressed and purified as described (Weiss et al., 1989). Recombinant dynamin 1 was kindly provided by Dr. H. Damke (The Scripps Research Institute). Mammalian Sec23/24 was purified from rat liver cytosol as described (Aridor et al., 1998). Mammalian Sec13/31 complex was partially purified from rat liver cytosol as described (Aridor et al., 1998).

Solubilization and Isolation of Sar1-VSV-G Complex from Microsome Membranes

The GTP-restricted GST-Sar1[H79G] (Sar1-GTP) mutant was added to urea-stripped VSV-infected microsomes and the membranes were incubated and collected as described (Aridor et al., 1998). Microsomal membranes were resuspended in transport buffer containing (mM) 20 Hepes, 70 KOAc, 1 MgOAc, and 250 sorbitol, and the reversible cross linker. 3′-dithiobissulfosuccimidylpropionate (DTSSP; 100 μM) was added. Membranes were incubated at room temperature for 15 min. The reactions were stopped by the addition of Tris HCl (pH 7.4, 50 mM final concentration) and membranes were collected by centrifugation. The membranes were solubilized in a buffer containing 50 mM Tris-HCl and 1% SDS supplemented with protease inhibitor cocktail for 15 min on ice. The solubilized membranes were centrifuged for 10 min at 7,500 rpm in a microfuge to remove insoluble material, and the resulting supernatant was diluted into a buffer containing (final concentration) 50 mM Tris-HCl, pH 7.4, 1% Triton X-100, 0.5% deoxycholate, 0.1% SDS, 150 mM NaCl, and a cocktail of protease inhibitors (RIPA). Solubilized membranes were incubated with affinity-purified antibodies to GST, covalently coupled to Protein A agarose beads for 1 h at 4°C and collected by brief centrifugation. The immunoprecipitate was washed four times with RIPA buffer and once with water before denaturation in Laemmli sample buffer supplemented with 50 mM DTT, and analyzed by SDS-PAGE and immunoblotting (Aridor et al., 1998). When reprecipitation was performed (see text), the isolated complex bound to anti–GST antibody and coupled to Protein A beads was washed twice with RIPA buffer and once with water, and resuspended in 50 mM Tris-HCl containing 1% SDS as described above. The complex was heated (55°C for 2 min) and separated from Protein A agarose beads by brief centrifugation. The resulting supernatant was diluted into RIPA buffer as described above and incubated with an anti–VSV-G monoclonal antibody (P5D4) covalently coupled to Protein G agarose beads for 1 h at 4°C. The resulting complex was collected by a brief centrifugation, washed four times with RIPA buffer and once with water, and analyzed using SDS-PAGE and immunoblotting or protein silver stain as described (Aridor et al., 1998).

Interaction of VSV-G Tail with Sar1

GST-VSV-G cytoplasmic tail (GST-tail) or GST fusion proteins with mutated cytoplasmic tails ([D21A] and [E23A]) or (19-24 A) or GST-mBet1 (amino acids 1–96) chimeras were generated, expressed in *Escherichia coli* and purified to homogeneity using GS-beads as described (Aridor et al., 1998). The GST fusion proteins or GST (4.5 μg each) were incubated with recombinant Sar1[H79G] or Sar1[T39N] (Sar1-GDP) (4 μg each) and/or purified Sec23/24 complex (4.5 μg) as described (Springer and Schekman, 1998) with the following modifications. The reaction was incubated at 32°C for 30 min before transfer to ice. Samples were incubated for 30 min in a reaction mixture containing 0.01% Triton X-100, 5 mM $MgCl_2$, 295 mM KOAc, 1 mM EDTA, 20 mM Hepes KOH, pH 7.4, 2% glycerol, 1 mM GTP (1 mM GDP when Sar1-GDP was used, see text), and 1 mM DTT in a final volume of 100 μl. GS-Sepharose beads were added and the mixture was incubated for additional 30 min at 4°C. GS beads were collected by brief centrifugation and washed as described (Aridor et al., 1998). The isolated complexes were analyzed on SDS-PAGE by immunoblotting using antibodies to Sar1 and Sec23 and stained with alkaline phosphatase.

Immunofluorescence Microscopy

Permeabilized cells (Plutner et al., 1992) were prepared and incubated with the indicated components as described in the figure legends. At the end of the incubations, the cells were fixed with 2% formaldehyde in phosphate buffered saline for 5 min, followed by a 1-min incubation with cold methanol (−20°C). For detergent extraction, permeabilized cells were transferred to ice at the end of the incubation and washed twice with KHM buffer as described (Plutner et al., 1992). Subsequently, the cells were incubated with KHM buffer supplemented with 0.5% Triton X-100 on ice for 1 min, washed with KHM, and fixed as above. Indirect immunofluorescence was performed as described (Plutner et al., 1992).

Image Analysis and Deconvolution Microscopy

Images were collected on a Delta Vision Optical Sectioning Microscope (No. 283) consisting of an Olympus IX-70 microscope equipped with a mercury arc lamp. A Photometrics CH 350 cooled CCD camera and a high precision motorized XYZ stage were used to acquire multiple consecutive optical sections at a 0.1–0.2-μm interval for each of the fluorescent probes. After data acquisition, the data was deconvolved using the DeltaVision software version 2.1 that is based on the Agard/Sadat inverse matrix algorithm. Each panel is a composite of the indicated number of sections from the middle of the cell.

Electron Microscopy

Immunoelectron microscopy and quantitation was performed as described (Bannykh et al., 1996). The gold labeling of ER-derived structures was specific as negligible labeling (<0.1 gold particles/μm membrane) was detected over mitochondria (not shown).

Imaging of Green Fluorescent Protein–VSV-G in Living Cells

Green fluorescent protein (GFP)–VSV-G was expressed in COS cells and visualized using time lapse video microscopy as described (Presley et al., 1997).

In Vitro Imaging Using Time-Lapse Video Microscopy

To analyze membrane extension, cells were permeabilized (Plutner et al., 1992) and labeled with $DiOC_6$ in KHM buffer for 20 min on ice (Dabora and Sheetz, 1988). After labeling, the cells were washed and incubated on a temperature-controlled stage. Cells were viewed on an IX-70 micro-

scope and video was recorded using a Panasonic GD-MF602 and Sony time-lapse video recorder (SVT-S3100), and processed using Adobe Premier 5.1 software for analysis. Images for differential interference contrast (DIC) analysis were similarly collected and analyzed from nonlabeled permeabilized cells. Mobilization of VSV-G in semi-intact cells was followed by video microscopy as described (Storrie et al., 1994) with the following modifications. Fab fragments of monoclonal antibody P5D4 were generated using immobilized papain (Pierce Chemical Co.) and separated from undigested IgG and Fc on immobilized Protein A column (Bio-Rad Laboratories). Fab fragments were labeled with Alexa 594 and separated from unconjugated dye by gel filtration according to the manufacturer's instructions (Molecular Probes Inc.). For labeling, permeabilized cells were incubated with labeled Fab for 20 min on ice before wash, followed by incubation on a temperature-controlled stage, and images were collected as described above.

Online Supplemental Materials

Online supplemental materials can be found at http://www.jcb.org/cgi/content/full/152/1/213/DC1.

Video 1 provides a three-dimensional view of Sar1 tubules labeled with DiOC, as in Fig. 5 A.

Video 2 shows a real-time video of the formation of tubules at ER export sites in living cells as described in Fig. 9.

Figure S1 used methods identical to Fig. 1 B, except that GST-Bet1 was used for recruitment instead of the GST-tail fusion protein to define its interaction with Sar1.

Figure S2 (A, 1–6) show mobilization of Fab-labeled VSV-G (Storrie et al., 1994) into Sar1-dependent tubules using deconvolution microscopy. The unprocessed, deconvolved image comprising five layers was collected at 90-s intervals. Note examples of extended tubule growth and retraction emanating from one focal origin point. Intense staining globular regions define perinuclear clusters of tubules containing VSV-G.

Figure S3 shows effect of MT-depolymerization on formation of Sar1-dependent tubules. In A–F, permeabilized cells were either not incubated (A and D), incubated for 30 min in the presence of Sar1-GTP (B and E), or incubated for 30 min with cytosol (C and F). Cells were fixed and labeled for MTs (anti–α-tubulin; A–C) or VSV-G (D–F) and images were collected using deconvolution microscopy. In G–I, cells were pretreated with colchicine for 2 h to depolymerize MTs prior to cell permeabilization. Subsequently, cells were incubated in the presence of Sar1–GTP alone (G and H) or cytosol (I) for 30 min. The distribution of VSV-G (G and I) or Sar1 (H) was determined using indirect immunofluorescence (Plutner et al., 1992). Figures are representative of at least three independent experiments. Bars, 5 μm. Note loss of tubule formation using cells in which MTs have been depolymerized prior to incubation in vitro.

Figure S4 shows the localization of kinesin to Sar1-GTP generated intermediates using cryoimmunoelectron microscopy. Cells incubated in the presence of cytosol and Sar1-GTP were prepared for cryoimmunoelectron microscopy as described (Bannykh et al., 1996) and the localization of kinesin (6-nm gold) using kinesin-specific antibody. Note the extensive tubular vesicular network juxtaposed to ER membranes that are typically formed under these incubation conditions. Bar, 100 nm.

Results

Sar1 Interacts with VSV-G on ER Membranes

Cargo selection from the ER into detergent-soluble prebudding complexes is one of the earliest detectable intermediates in ER-to-Golgi transport. Selection is mediated by the activation of the Sar1 GTPase and the subsequent recruitment of the Sec23/24 subunits of the COPII coat (Aridor et al., 1998; Kuehn et al., 1998). To more precisely define the role of Sar1 in the initial events governing ER export, VSV-G-containing ER microsomes were washed to remove endogenous COPII components (Aridor et al., 1998) and incubated in the presence of a recombinant GST-tagged activated form of the Sar1 GTPase (Sar1[H79G], designated GST-Sar1-GTP). GST-Sar1-GTP is fully functional in supporting COPII vesicle budding in vitro (Aridor et al., 1998). After incubation, microsomes were transferred to ice, incubated with the reversible cross-linker DTSSP, and then solubilized under denaturing conditions in the presence of SDS. In the presence of cross linker, VSV-G was readily recovered by immunoprecipitation with a GST-specific antibody in a GST-Sar1-GTP containing complex (Fig. 1 A, b). Recovery was specific as no VSV-G was observed in the absence of GST-Sar1-GTP (Fig. 1 A, a) and ribophorin II, an abundant ER protein, was excluded from the cross-linked immunocomplex (Fig. 1 A, f and g), as previously observed for prebudding complexes (Aridor et al., 1998; Kuehn et al., 1998). VSV-G recovery under denaturing conditions was largely dependent on cross linking, although a small amount was recovered in the absence of cross linker (Fig. 1 A, c). Binding was not observed when membranes were retained on ice (Fig. 1 A, d), demonstrating that recruitment occurred only under physiological conditions that support Sar1 activation through the Sec12 exchange factor leading to COPII vesicle formation (Aridor et al., 1995, 1998; Aridor and Balch, 1996, 2000). Finally, although Sar1 is present in a large excess to VSV-G on the membranes (Aridor et al., 1998), when the Sar1 immunoprecipitate was denatured with SDS and reprecipitated with an antibody specific for VSV-G, we could show in silver-stained gels that the cross-linked GST-Sar1 was recovered in comparable levels to VSV-G (Fig. 1 A, i). The identity of the bands was verified by immunoblotting (not shown). Together, these data suggest that Sar1 interacts with cargo and initiates the recruitment of VSV-G into prebudding complexes.

Sar1 Can Interact Directly with the VSV-G Cytoplasmic Tail and Initiate COPII Coat Assembly in an Exit Code–specific Manner

To determine if VSV-G can interact directly with Sar1, we analyzed the ability of a fusion protein in which the cytoplasmic tail of VSV-G was linked to GST (GST-VSV-G tail) to bind purified Sar1 (Fig. 1 B). Incubation of the GST-VSV-G tail with Sar1-GTP led to efficient recovery of the Sar1 GTPase on glutathione-Sepharose (GS) beads (Fig. 1 B, c). Binding did not require Sar1 activation as the inactivated, GDP-restricted form (Sar1[T39N]; Sar1-GDP), which will not support COPII coat recruitment to ER membranes (Aridor et al., 1995, 1998; Rowe et al., 1996), was also recovered on beads (Fig. 1 B, g). No binding was observed by GST alone (Fig. 1 B, a, b, and f), attesting to the specificity for binding to the VSV-G cytoplasmic tail. VSV-G bound to Sar1 can support coat assembly as the binding of Sar1-GTP, but not Sar1-GDP, to the tail led to the recruitment of Sec23/24 to beads (Fig. 1 B, d and h, respectively). Thus, the VSV-G tail does not recognize the Sec23/24 complex directly under these conditions (Fig. 1 B, e). As has been observed for yeast Sar1p (Springer and Schekman, 1998), similar interactions with Sar1 and Sec23/24 were observed when a GST fusion protein containing the cytosolic portion (amino acids 1–96) of the mammalian SNARE Bet1 was used (see Fig. 1S, online supplement).

To further define the specificity of Sar1 interaction with VSV-G and to correlate it with the established role for an exit code in the cytoplasmic tail for export of VSV-G from the ER, we analyzed the ability of Sar1 to interact with a mutated cytoplasmic tail of VSV-G and to recruit COPII

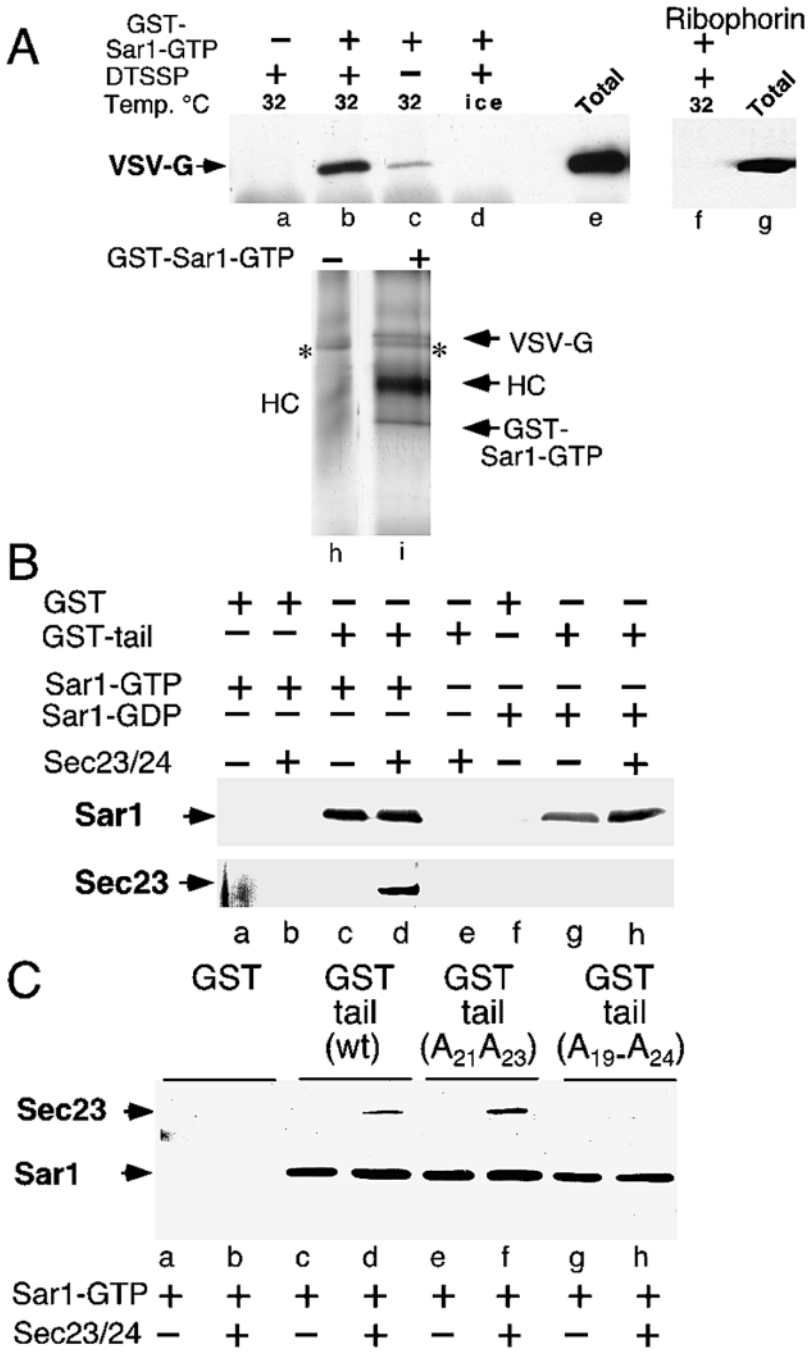

Figure 1. Sar1 interacts with the VSV-G cytoplasmic tail and assembles COPII coats in an export signal-dependent manner. (A, a–e) VSV-G containing ER microsomes were incubated as described (Rowe et al., 1996) in the absence (a) or presence (b–d) of GST-Sar1-GTP, on ice (d) or at 32°C (a–c) for 30 min, before transfer to ice and incubation in the absence (c) or presence (a, b, and d) of the reversible cross linker DTSSP. Subsequently, membranes were solubilized in detergent buffer and the lysate was incubated with anti–GST antibody. The amount of VSV-G (a–e) or ribophorin (f and g) recovered in the immunoprecipitate was determined by immunoblotting with specific antibody (Aridor et al., 1998). e shows 25% of the total VSV-G present in the incubation. h and i show a silver-stained gel used to determine the stoichiometry of the GST-Sar1/VSV-G complex. ER microsomes were incubated as described above in the absence (h) or presence of GST-Sar1-GTP (i). The cross-linked complex was isolated by immunoprecipitation with anti–GST antibodies, denatured in the presence of 0.1% SDS at 55°C, and reisolated with VSV-G-specific antibody and analyzed by SDS-PAGE. The location of the antibody heavy chain remaining associated with denatured GST-Sar1-VSV-G complex is indicated (HC). *Nonspecific band recovered under both incubation conditions. VSV-G and Sar1 were identified in a duplicate gel analyzed by immunoblotting (not shown). (B) GST (a and b) or the GST-VSV-G (GST-tail) fusion protein were incubated with purified Sar1-GTP (a–d) or Sar1-GDP (f–h) in the absence (a, c, f, and g) or presence (b, d, e, and h) of purified Sec23/24 complex as described. The amount of Sar1 (top) or Sec23 (bottom) recovered on GS beads was determined by immunoblotting with specific antibody. (C) GST or GST-tail fusion proteins containing either the wild-type 29 amino acid tail of VSV-G (wt) (YTEIDM at positions 19–24), a mutant harboring a D21A and E23A substitution ($A_{19}A_{21}$), or Ala substitutions for the entire export signal ($A_{19\text{-}24}$) were incubated with Sar1-GTP and purified Sec23/24 proteins as indicated, and the recovery of Sar1 or Sec23 was determined as described above. Figures are representative of at least four independent experiments.

components onto GS beads. We previously demonstrated that alanine substitution of the DXE motif ($D_{21}XE_{23}$ to $A_{21}XA_{23}$) on the VSV-G cytoplasmic tail abolishes VSV-G concentration, leading to a reduction of the half time ($t_{1/2}$) of VSV-G transport from the ER to the Golgi from 10–20 to 45–60 min (Nishimura et al., 1998, 1999). Recent analysis demonstrated that the ER export motif also includes flanking amino acids 19-YTDIEM-24 (Sevier et al., 2000), where alanine substitution ($A_{19\text{-}24}$) led to further reduction of VSV-G transport to a $t_{1/2}$ of 125–150 min (Nishimura and Balch, 1997; Sevier et al., 2000). This complete motif is necessary and sufficient to support ER export of cargo (Bannykh et al., 1998; Sevier et al., 2000).

Recombinant GST chimeras that contain the VSV-G tail with the $A_{21}XA_{23}$ substitution (Nishimura and Balch, 1997) or the entire $A_{19\text{-}24}$ substitution (Sevier et al., 2000) were produced and analyzed for their ability to interact with Sar1 and to assemble COPII coat on GS beads. Under these conditions, we found that Sar1 interacts with similar efficiency with both the wild-type and the $A_{21}A_{23}$ VSV-G tails. In both cases, Sar1-GTP binding led to recruitment of the Sec23/24 complex (Fig. 1 C, c–f). This result is in agreement with our recent demonstration that VSV-G containing the $A_{21}A_{23}$ mutation is efficiently collected by Sar1 and Sec23/24 into prebudding complexes and that incubation of VSV-G($A_{21}A_{23}$)-expressing cells with excess Sar1-GTP in vitro can effectively reverse the concentration deficiency of the $A_{21}A_{23}$ mutant (Nishimura et al., 1999).

The $A_{19\text{-}24}$ tail was also capable of efficiently recruiting Sar1 (Fig. 1 C, h). However, in contrast to the $A_{21}A_{23}$ mu-

tant, the $A_{19\text{-}24}$ mutant was markedly deficient in its ability to support Sec23/24 recruitment (Fig. 1 C, compare f with h). As the Sec23/24 complex by itself fails to bind the wild-type VSV-G tail (Fig. 1 B, e), its ability to be recruited to the GST tail in an exit-code and Sar1-dependent manner suggests that interaction and activation of Sar1 with ER cargo may impose a conformational change in Sec23/24 that allows it to interact with export signals. Thus, Sar1 promotes cargo–Sec23/24 interaction in the ternary complex. These results could explain the observed cooperativity of Sar1 and Sec23/24 in cargo selection of VSV-G during the formation of prebudding complex on ER membranes (Aridor et al., 1998) and suggest a role for Sar1 in the initial recognition of the ER export signal.

Sar1 Mobilizes Cargo into Tubular Domains in the ER

Given the possible role for Sar1 in initiating cargo recognition, we next determined whether we could detect novel morphological intermediates that precede assembly of the COPII coat. For this purpose, we used an assay that reconstitutes the synchronized, COPII-dependent export of tsO45 VSV-G from the ER in semi-intact cells (Plutner et al., 1992; Aridor et al., 1998).

Permeabilized normal rat kidney (NRK) cells containing VSV-G exclusively in the ER were washed to remove endogenous membrane-bound Sec23/24 components and incubated in vitro (Aridor et al., 1998). In the absence of cytosol, VSV-G remained in the ER (Fig. 2 A), reflecting the requirement for recruitment of the cytosolic COPII budding machinery (Plutner et al., 1992; Kuge et al., 1994; Aridor et al., 1995). In the presence of cytosol, VSV-G was transported to numerous punctate structures (Fig. 2 B) previously identified as VTCs that form after COPII budding (Saraste and Svensson, 1991; Bannykh et al., 1996). Incubation of cytosol together with Sar1-GTP also led to the mobilization of VSV-G into these punctate structures, albeit at reduced efficiency (Fig. 2 C) (Aridor et al., 1995). Previous studies have established that, due to the ability of the activated Sar1-GTP to inhibit COPII uncoating, the COPII-coated vesicles fail to develop into mature VTCs

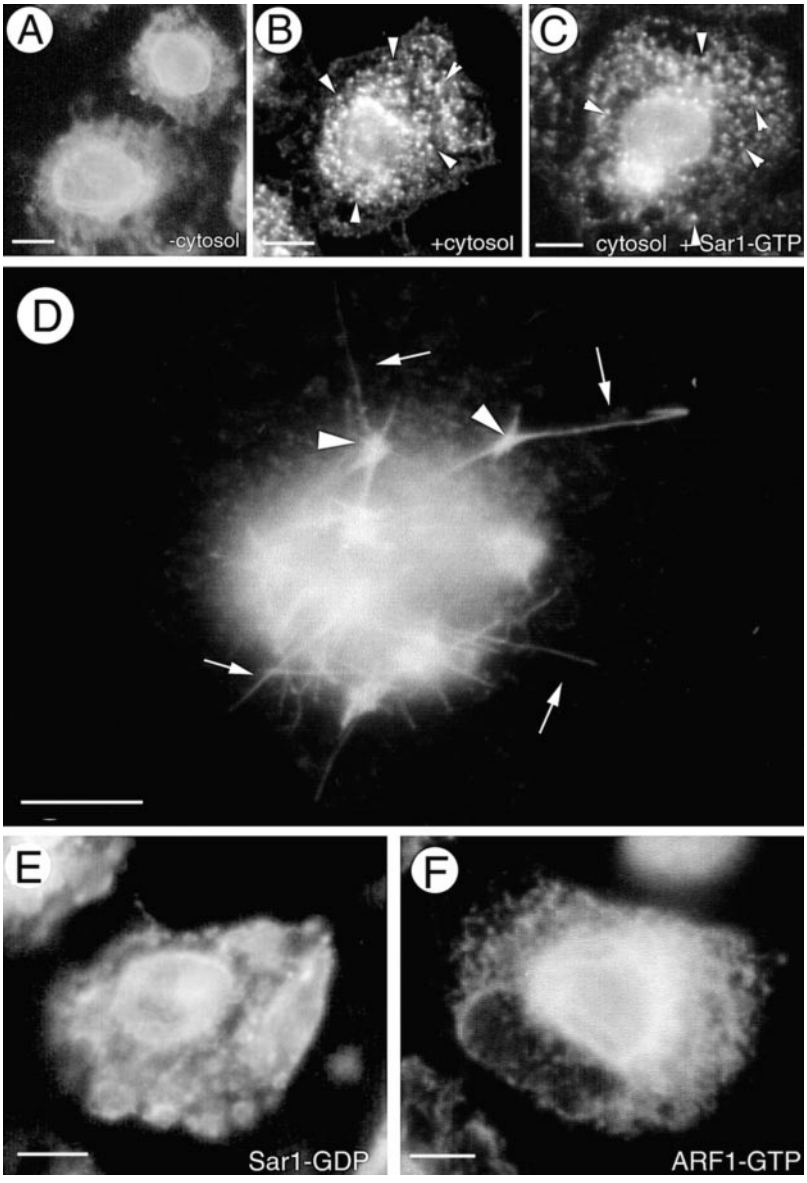

Figure 2. Sar1-GTP triggers the formation of VSV-G-containing tubules. Permeabilized NRK cells (Plutner et al., 1992) were incubated either in the absence (A) or presence (B) of cytosol, with cytosol and 10 μg Sar1-GTP (C), with Sar1-GTP only (D), with Sar1-GDP only (E), or with activated ARF1 (ARF1-GTP) only (F), in 220 μl for 30 min at 32°C as described in Materials and Methods. The distribution of VSV-G was determined using indirect immunofluorescence with specific antibody (Plutner et al., 1992). The arrowheads in B and C denote punctate VTCs. The arrows in D denote tubules containing accumulated VSV-G; the arrowheads denote foci of tubule formation. All figures are representative of at least five independent experiments. Scale bar: 5 μm.

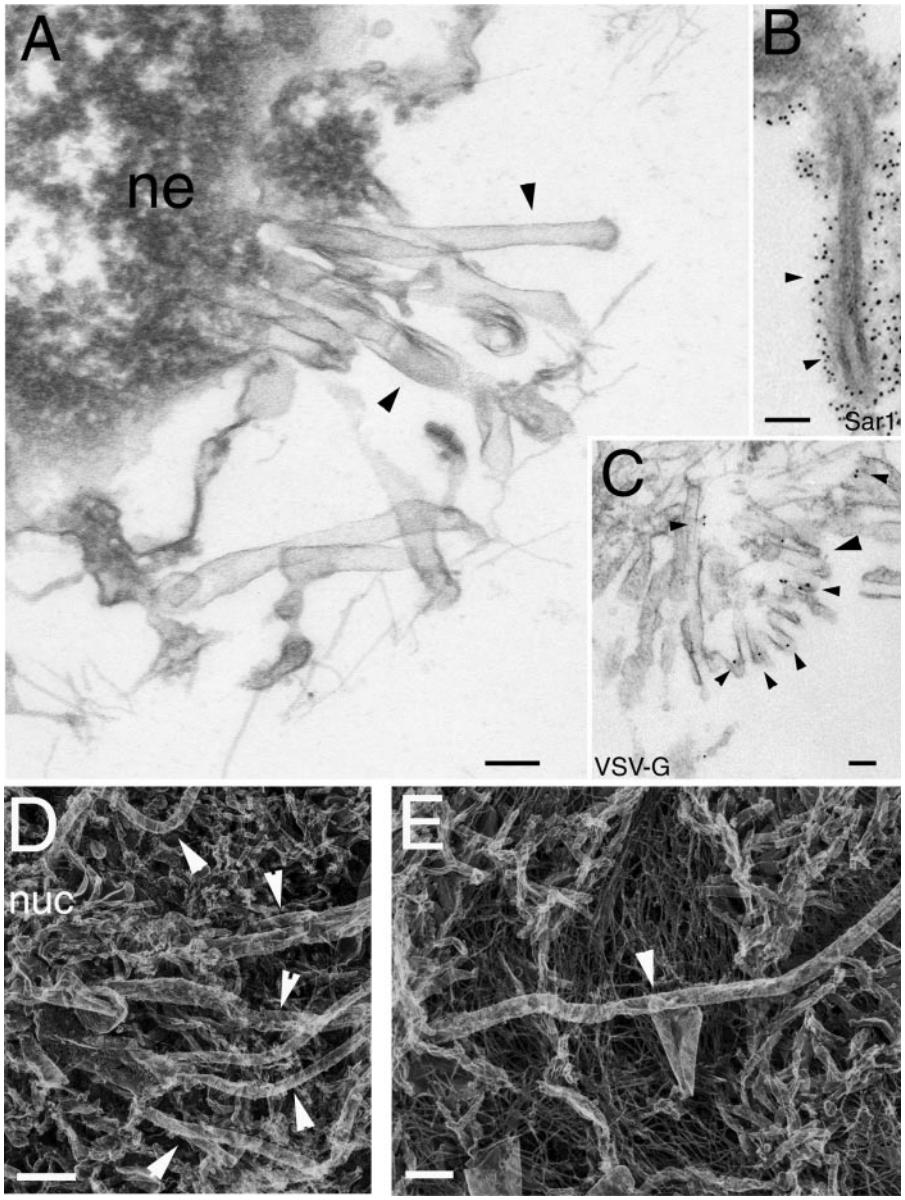

Figure 3. Electron microscopy analysis of Sar1-dependent tubular domains. (A–C) Permeabilized cells were incubated as described in Fig. 2 in the presence of Sar1-GTP, and prepared for EM as described (Bannykh et al., 1996). In A, a typical image of Sar1-dependent tubules (arrowheads) forming at a focal point on the nuclear envelope (ne) at early time points. In B, Sar1-dependent tubules are immunolabeled with specific antibody for Sar1 (arrowheads) and detected with 10 nm gold-labeled secondary antibodies. In C, a cluster of tubules (large arrowhead) is immunolabeled with 6 nm gold for VSV-G (arrowheads). (D and E) Quick-freeze, deep-etch micrographs of permeabilized cells incubated in the presence of Sar1-GTP as described in Fig. 2. Arrowheads show 40–80-nm tubular elements that are formed in response to Sar1 activation. Scale bar: 100 nm.

and appear attached to each other as "beads on a string" confined to ER export sites (Bannykh et al., 1996).

In striking contrast to the above results, when incubations were performed in the presence of activated Sar1-GTP alone, VSV-G was collected into long tubular elements. These extended up to 14 μm towards the cell periphery (Fig. 2 D). Identical results were observed when cells were incubated in the presence of wild-type Sar1 and GTP (see below, Fig. 7). In this case, the absence of the Sec23/24 complex that functions as a Sar1 GTPase-activating protein prevents wild-type Sar1 from hydrolyzing bound GTP (Aridor et al., 1998), leading to accumulation of Sar1 in the GTP-bound state on membranes.

When imaged at high resolution using electron microscopy (Fig. 3), tubules were found to have a striking morphology with multiple ~40–80-nm tubular elements emanating from defined foci on the surface of the nuclear envelope and ER elements (Fig. 3 A). Immunoelectron microscopy (Fig. 3 B) revealed that tubules had an extensive surface coat of Sar1 with an 18-fold higher linear density than that found on the ER (Sar1 coated tubules, 37 ± 4.2 gold particles/μm membrane; ER, 2 ± 0.2 gold particles/μm membrane). Tubules and tubule clusters contained VSV-G based on immunocytochemistry using HRP staining (not shown). Immunogold labeling (Fig. 3 C) revealed that VSV-G was concentrated on ER-connected tubules (5 ± 2 gold particles/μm), as compared with ribosome-studded regions of the ER (1 ± 0.5 gold particles/μm membrane). When imaged using quick-freeze, deep-etch methodologies (Heuser and Keen, 1988) (Fig. 3, D and E), tubules observed in Sar1-containing incubations, but not in control incubations, were similar in diameter to ER transitional elements observed in vivo (Palade, 1975; Bannykh et al., 1996; Aridor et al., 1999). These results suggest that recruitment of activated Sar1, in the absence of other cytosolic COPII components, can initiate cargo selection and form a Sar1-coated domain on tubular extensions of the ER.

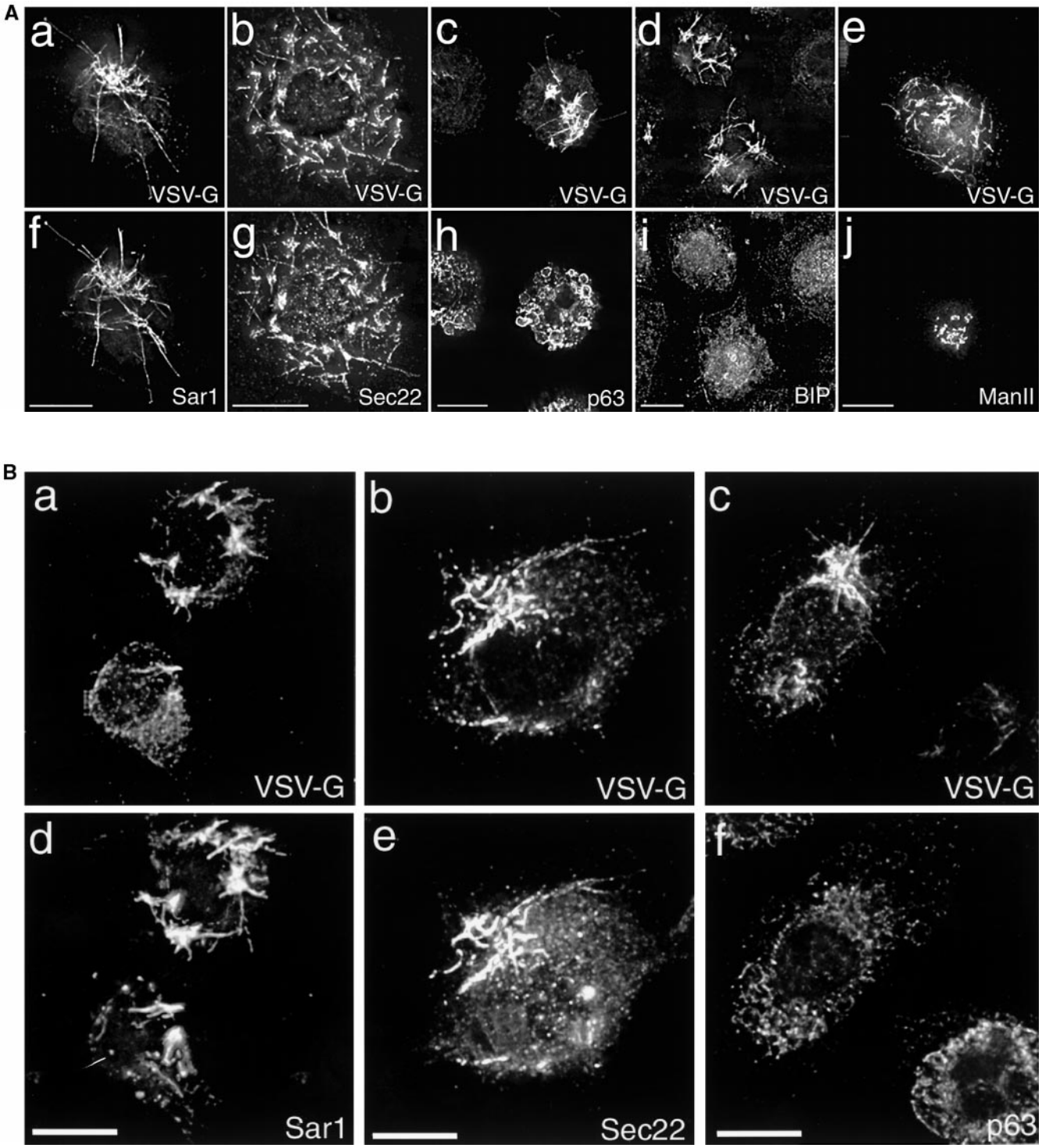

Figure 4. A selective domain containing cargo is formed from the ER after Sar1 activation. (A) Permeabilized NRK cells were incubated in the presence of Sar1-GTP as described above, and the distribution of VSV-G (a–e) was compared with that of Sar1 (f), Sec22 (g), p63 (h), BIP (i), and Man II (j) using indirect immunofluorescence. VSV-G colocalized with Sar1 (a and f) and the cargo SNARE protein Sec22 (b and g), but not with the resident ER membrane protein p63 (c and h), the resident soluble ER protein BIP (d and i), or Man II (e and j). Figures are representative of at least four independent experiments. Scale bar: 15 μm. (B) Sar1-dependent ER tubular domains are detergent resistant. After incubation of permeabilized cells in the presence of Sar1-GTP, the cells were extracted with ice-cold Triton X-100 as described in Materials and Methods before fixation and analysis using indirect immunofluorescence. Sar1-coated tubules (d) resist the detergent extraction and retain the cargo proteins VSV-G (a–c) and Sec22 (e), while the resident ER membrane protein p63 is largely extracted (f) (compare with the nonextracted condition shown in A, h). Shown are deconvolved images. Figures are representative of at least four independent experiments. Scale bar: 15 μm.

Sar1-mediated Tubule Formation Requires Sar1 Activation

We next analyzed the requirement for Sar1 activation in the formation of the tubular domain and the specificity of this reaction. VSV-G-containing tubules were not observed when permeabilized cells were incubated on ice in the presence of Sar1-GTP (not shown), nor in the presence of Sar1-GDP (Fig. 2 E). The formation of ER-derived tubules was specific for Sar1. Tubules were not observed when cells were incubated in the presence of the GTP-restricted form of myristoylated ARF1 (ARF1-GTP) (Fig. 2 F), a GTPase specific for the assembly of retrograde COPI vesicles from VTCs and the cis Golgi (Cosson and Letourneur, 1997; Allan and Balch, 1999), nor were they observed in the presence of recombinant dynamin 1 (not shown) that can tubulate the plasma membrane and synthetic liposomes in vitro (Takei et al., 1998). Together, these data establish that tubule formation requires Sar1 activation on ER membranes.

Sar1-mediated Tubules Selectively Collect Cargo

Cargo collected into Sar1-GTP–triggered tubules was selective as the abundant ER resident soluble protein BIP (Fig. 4 A, i) or the resident membrane ER protein p63 (Fig. 4 A, h) were not collected into VSV-G-containing tubules (Fig. 4 A, c and d). Identical results were observed for the resident ER proteins calnexin and kinectin (not shown). Furthermore, no overlap was observed between VSV-G and the cis/medial Golgi marker protein Man II (Schwaninger et al., 1991; Velasco et al., 1993) (Fig. 4 A, e and j), indicating that Sar1 tubule formation is restricted to its normal site of function, the ER. However, VSV-G did show striking overlap with Sar1-GTP (Fig. 4 A, a and f), a result that is in agreement with the immunoelectron microscopy. Similarly, another membrane cargo, the SNARE protein Sec22, which is selected into prebudding complexes (Aridor et al., 1998) and exported from the ER in COPII vesicles (Rowe et al., 1996, 1998; Allan et al., 2000) was also collected into these Sar1 domains (Fig. 4 A, b and g). In the same experiment, we found that tubules resist extraction by ice-cold Triton X-100 as Sar1, VSV-G, and Sec22 remain on the coverslip in intact, overlapping tubular structures (Fig. 4 B, compare a with d and b with e). In contrast, the ER protein p63 that was abundant in swollen ER membranes but not in Sar1 tubules before treatment with Triton X-100 (Fig. 4 A, c and h) was largely extracted by detergent (B, f). Thus, Sar1, VSV-G, and Sec22 are clearly localized in tubular structures that comprise a separate entity connected to the ER. We conclude that the observed tubules define specialized protein domains in the ER that are formed after Sar1 activation to initiate membrane cargo selection.

Real-Time Visualization of Sar1 Tubule Growth and VSV-G Movement Using Fluorescence Video Microscopy

Sar1 tubules containing Sec22 (Fig. 4 A, g) were also observed to form in noninfected cells incubated in the presence of Sar1-GTP (not shown). Thus, tubule formation was not dependent on the presence of VSV-G. We therefore analyzed Sar1 tubule formation in real time in noninfected permeabilized cells. To visualize ER-connected structures, the cells were preincubated with the cationic fluorescent dye, $DiOC_6$, that specifically labels the ER (Terasaki and Reese, 1992). After labeling, the cells were washed and incubated in the presence of activated Sar1. Under these conditions, we observed a striking collection of $DiOC_6$-stained tubular extensions (Fig. 5 A).

To determine the rate of tubule elongation in $DiOC_6$-stained cells, we used time-lapse video microscopy of whole-cell images (Fig. 5, B1–B8). Sar1-dependent, $DiOC_6$-labeled tubular elements formed at numerous sites along the ER located throughout the cytoplasm, consistent with results presented for VSV-G-labeled tubules shown in Figs. 2 and 3, and characteristic of the random distribution of ER export complexes involved in the formation of VTCs (Bannykh et al., 1996). $DiOC_6$-containing tubules were formed in a saltatory fashion with stationary periods and elongated on a linear path. No intersections or net formation (three-way membranes), which represent ER membrane fusion events observed during formation of the reticular ER (Dabora and Sheetz, 1988; Dreier and Rapoport, 2000) were detected. During elongation of tubules at the cell periphery (where imaging was sufficiently clear to delineate individual tubules), we recorded bursts of movement of up to 0.5 μm/s (Fig. 5, B1–B8). Cargo accumulation into growing tubules can also be followed in nonfixed cells. For these experiments (see Fig. 2S, online supplement), VSV-G was tagged with fluorescently labeled Fab fragments prepared from an anti–VSV-G cytoplasmic tail antibody, as was previously used to follow movement of VSV-G in vivo (Storrie et al., 1994).

Given the potential deleterious effects of long-term fluorescence recording on cellular functions and the difficulty of imaging the formation $DiOC_6$ fluorescent tubules within the cell body, we also used DIC microscopy to analyze the rate of tubule elongation (Fig. 5, C1–C8). Under these conditions, we observed temporal bursts of elongation of Sar1-coated tubules within the cell body at rates of up to 1.5 μm/s. The observed rates of tubule elongation (0.5–1.5 μm/s) are compatible with rates reported for either microtubule-dependent motors, such as kinesin or dynein, or the slower actin-based motor, myosin V. Each of these motors has been implicated in mediating or supporting expansion of the ER reticular network or in ER positioning within the cell (Dabora and Sheetz, 1988). Similar rates have also been recorded for the dynein-promoted movement of VTCs between the ER and the Golgi (Presley et al., 1997; Lane and Allan, 1999). We found that disruption of microtubules with either colchicine or nocodazole inhibited Sar1-mediated tubule formation (see Fig. 3S, online supplement); however, no obvious colocalization of Sar1 tubules with MTs was observed (not shown). Thus, involvement of MTs may occur only through interactions at the tips of the growing tubules, or it may be indirect.

We next analyzed the distribution and number of membrane tubules formed in the cell using optical sectioning and deconvolution microscopy to reconstruct the cell architecture in three dimensions (see three-dimensional reconstruction in Movie 1 in the supplemental material). As observed in fixed cells, tubules were formed at numerous sites throughout the cell. More than 120 clearly visible tubules and tubule initiation sites could be identified within the cell. This number is compatible with the number of ER export sites in the cytoplasm detected in vivo under similar

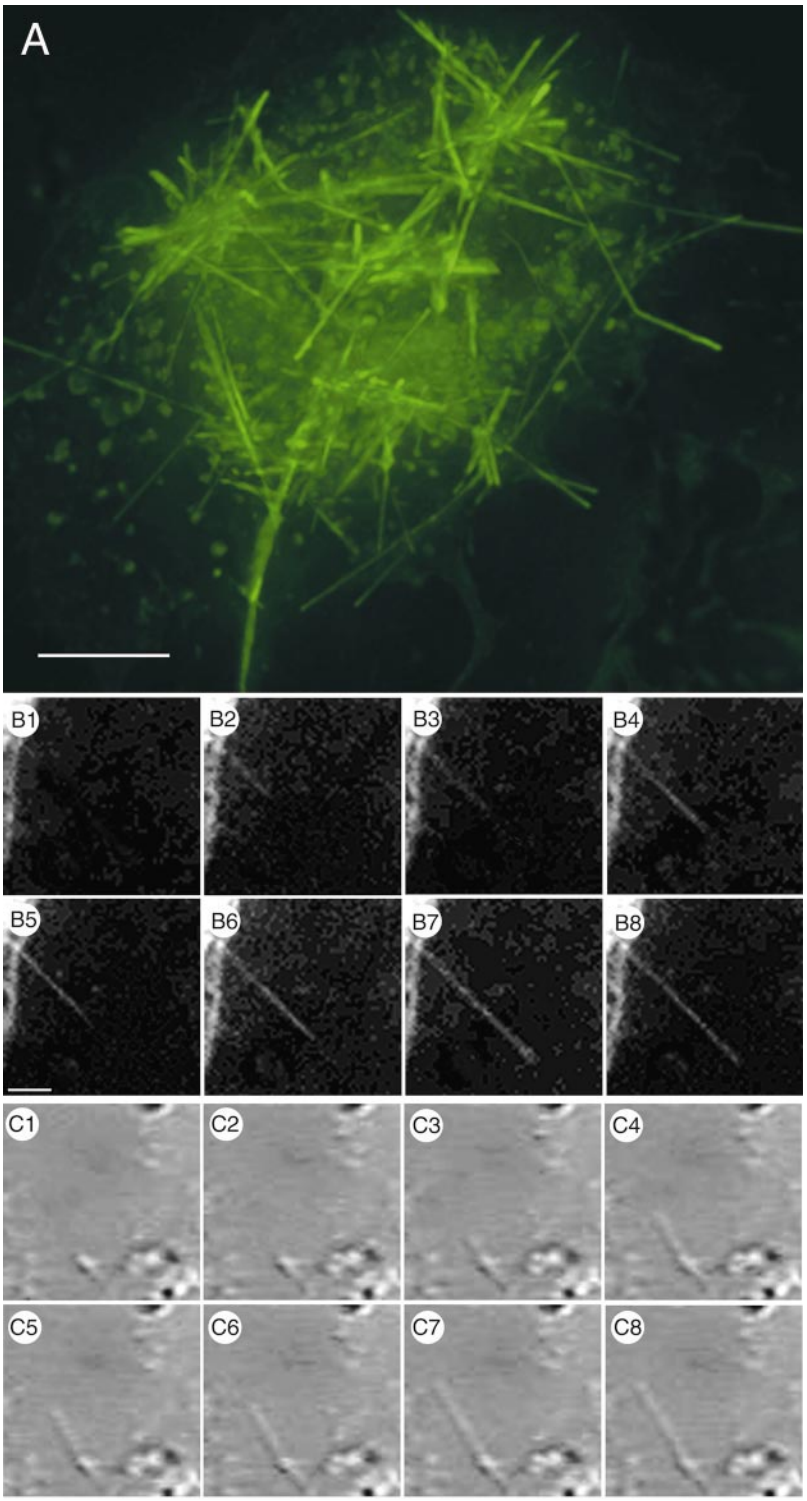

Figure 5. Formation and elongation of Sar1-dependent tubules. Permeabilized NRK cells were labeled with $DiOC_6$, washed, and incubated with Sar1-GTP. $DiOC_6$ fluorescence (A and B) or video-enhanced DIC (C, see below) were used to follow Sar1-dependent tubule formation (Allan and Vale, 1994). Deconvolution microscopy (A) was used to generate a three-dimensional reconstruction of a $DiOC_6$-labeled cell from 36 sections, 0.2-μm each (scale bar: 5 μm). More than 120 tubules are visible within the cell (for full three-dimensional reconstruction, see Movie 1 in the supplemental material). The faint outline delimits the cell boundary. Tubule elongation in $DiOC_6$-labeled cells was monitored in real time. B1–B8 show continuous images taken at 4-s intervals to follow elongation of a single tubule. Elongation rates observed were B1–B2, 0.55 μm/s; B2–B3, 0.3 μm/s; B3–B4, 0.3 μm/s; B4–B5, 0 μm/s; B5–B6, 0.45 μm/s; B6–B7, 0.38 μm/s; B7–B8, 0 μm/s. (C) DIC was used to follow Sar1-induced tubule elongation in unlabeled cells. C1–C8 depict 1.25-s interval recordings of the elongation of a single tubule. Observed rates are C1–C2, 0.264 μm/s; C2–C3, 0.824 μm/s; C3–C4, 1.48 μm/s; C4–C5, 0.056 μm/s; C5–C6, 0.396 μm/s; C6–C7, 1.3 μm/s; C7–C8, −0.18 μm/s. Scale bar: 2 μm for B and C (shown in B5).

conditions (Aridor et al., 1995, 1999; Bannykh et al., 1996). Therefore, we suggest that activated Sar1 mediates the formation of bona fide ER export sites whose structure is exaggerated in the absence of other COPII components.

The Microtubule Motor Kinesin Is Recruited to Sar1-GTP Intermediates

Sar1-dependent formation of elongated tubules is dependent on the integrity of microtubules (Fig. 3S). Moreover, the rates measured for tubule elongation suggested the involvement of MT motors (Fig. 5). To determine whether activated Sar1 can recruit microtubule motor proteins, permeabilized cells were incubated in the presence of Sar1-GTP and the absence of cytosol to promote tubule growth. Under these conditions, the cell membrane–associated pools of kinesin and dynein provide a source of protein. While we detected minimal association of dynein (Fig. 6, A1–A3), the motor kinesin was more clearly detectable on the Sar1-GTP-generated intermediates (Fig. 6, D1–D3).

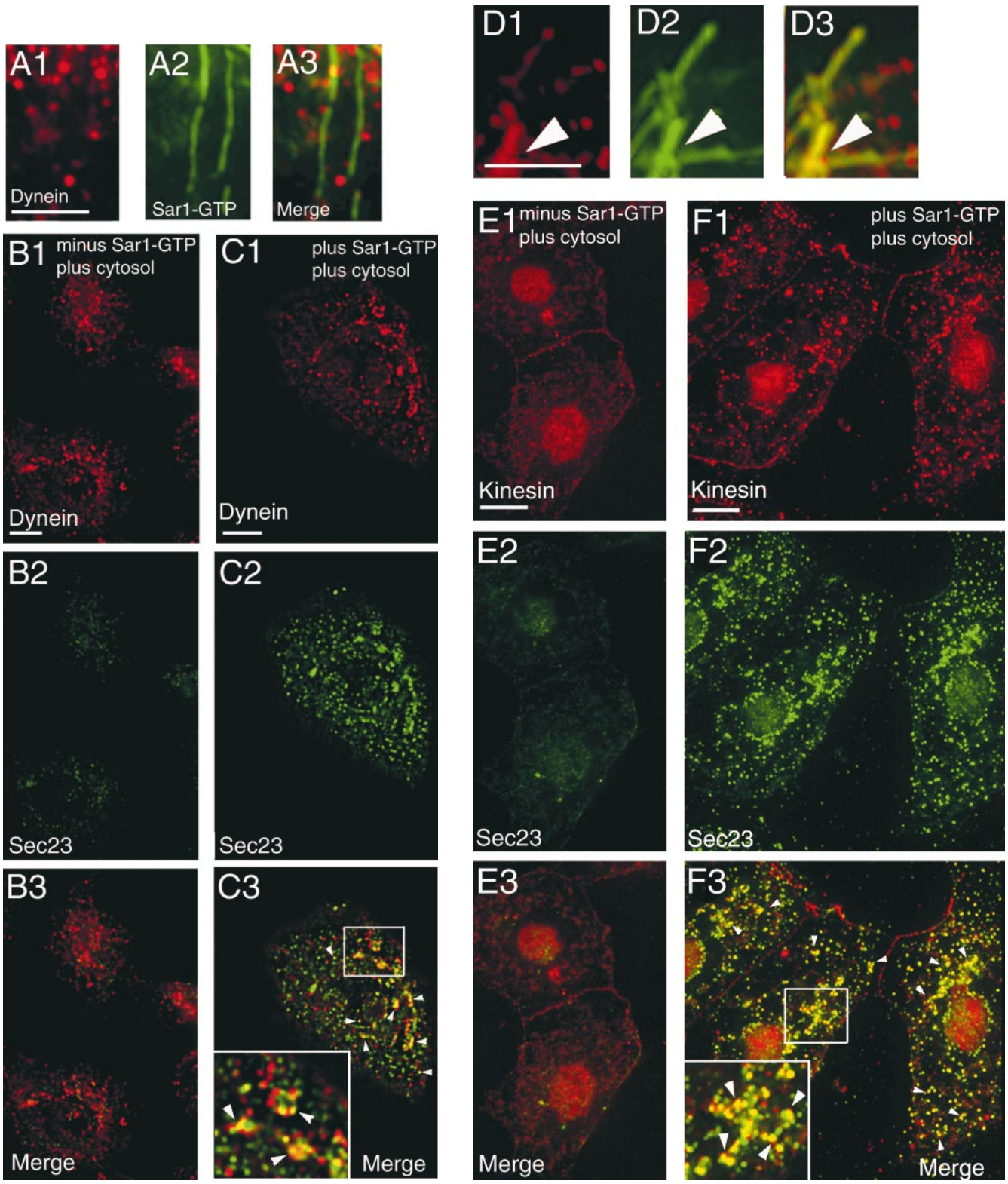

Figure 6. Sar1-dependent recruitment of microtubule motors. Permeabilized NRK cells were incubated with (B–C and E–F) or without (A and D) cytosol in the presence (A, C, D, and F) or absence (B and E) of Sar1-GTP for 30 min at 32°C. Cells were fixed and stained for dynein (using a 70.1 anti-intermediate chain antibody; A1, B1, and C1), kinesin (using the H1 anti-kinesin heavy chain antibody; D1, E1, and F1), Sar1 (A2 and D2), and Sec23 (B2, C2, E2, and F2). A–F3 show merged results of separate corresponding images. A1–A3 are compiled from 16 0.2-μm optical sections; B1–B3 are compiled from 8 0.2-μm sections; C1–C3 are compiled from 9 0.2-μm sections; D1–D3 are compiled from 11 0.2-μm sections; E1–E3 are compiled from 12 0.2-μm sections; and F1–F3 are compiled from 20 0.2-μm sections. Note that addition of activated Sar1 (Sar1-GTP) in the presence of cytosol leads to robust recruitment of Sec23 (C2 and F2) and specific mobilization of kinesin-to-ER export domains coated by Sec23 (F3). Scale bars: 5 μm.

Because cytosol can provide a more abundant source for microtubule motors than membranes, we repeated the above experiments in the presence of cytosol to assess the affect of Sar1-GTP on motor recruitment under more physiological conditions that lead to the generation of normal ER to Golgi intermediates. The amount of intermediate formation was determined by visualization of Sec23 recruitment to membranes (Aridor et al., 1995, 1998; Bannykh et al., 1996; Rowe et al., 1996). In controls performed in the absence of Sar1-GTP, incubation of permeabilized cells with cytosol led to only limited stabilization of Sec23 on ER membrane (Fig. 6, B2 and E2) due to the rapid uncoating activity of nascent COPII vesicles and transport of cargo to the Golgi (Aridor et al., 1995). Moreover, there was no detectable colocalization with either kinesin or dynein with Sec23-containing structures under these conditions (Fig. 6, B3 and E3). However, incubation of the cells and cytosol in the presence of activated Sar1-GTP led to stable recruitment of Sec23 to punctate structures throughout the cell comprising clusters of COPII intermediates (Fig. 6, C2 and F2) (Bannykh et al., 1996; Aridor et al., 1998, 1999). The presence of Sar1-GTP did not significantly affect the distribution of dynein (Fig. 6, compare B1 with C1) with <25% punctate structures containing Sec23 showing positive overlap with dynein (Fig. 6, C3). In striking contrast, kinesin was specifically recruited by incubation in the presence of Sar1-GTP (Fig. 6, compare E1 with F1) and showed strong overlap with Sec23-containing punctate structures (>80%) (Fig. 6, F3). Kinesin could also be readily detected on intermediates formed in the presence of Sar1-GTP using immunoelectron microscopy (see Fig. 4S, online supplement). Hence, under physiological conditions, activation of Sar1 leads not only to the recruitment of functional COPII coat components, but couples these events to the recruitment of the microtubule-motor kinesin, consistent with the dependence of Sar1-tubule growth on microtubules (Fig. 3S).

Sar1 Generated Tubules Are Functional Intermediates in ER Export In Vitro

If Sar1-mediated tubule formation does in fact represent a functional early intermediate in ER export, then they should be able to mediate later events in ER-to-Golgi transport. To visualize the completion of the ER export step in cells following Sar1 activation, tubule formation, and recruitment of VSV-G, we examined the fate of Sar1-dependent tubules morphologically after the addition of COPII components to permeabilized cells using a two-stage assay. Permeabilized cells were first incubated in stage 1 with Sar1-GTP for 30 min at 32°C to accumulate extended cargo-containing tubules. Purified COPII components Sec23/24 and Sec13/31 were subsequently added in the absence of additional Sar1, and the cells were incubated in stage 2 for 10 min at 32°C to promote ER export. The distribution of VSV-G and Sar1 under each of these conditions was examined using deconvolution fluorescence microscopy (Fig. 7 A).

In the presence of Sar1-GTP alone (stage 1), numerous extended VSV-G-containing Sar1-coated tubules emanating from multiple foci could be detected (Fig. 7 A, a–c, arrows). Addition of the COPII components Sec23/24 and Sec13/31 in the second stage resulted in a qualitative shortening of the tubular structures, as observed by Sar1 staining (Fig. 7 A, d). VSV-G that was present in the ER or accumulated in Sar1-coated tubular elements at the beginning of the incubation (Fig. 7 A, b) was recovered in numerous punctate structures (Fig. 7 A, e). Some VSV-G-containing structures were associated with the nuclear envelope and lacked overlap with Sar1 (Fig. 7 A, f). These are likely to represent VTCs forming directly from the ER in the second-stage incubation. However, numerous VSV-G-containing punctate elements clearly showed overlap with the disassembling Sar1 tubules (Fig. 7 A, f; small arrows). Higher magnification images of these structures revealed that VTCs were continuous with the Sar1-coated tubules (Fig. 7 A, f; large arrowheads show location of insets 1–4).

The formation of VSV-G-containing punctate foci could also be observed using time-lapse video microscopy. In these images (Fig. 7 B, 1–4, arrowheads), VSV-G labeling can be seen to increase in intensity upon incubation of Sar1-GTP–dependent tubules in the presence of purified Sec23/24 and Sec13/31 components. This result is consistent with our previous observations that Sec23/24 increases (20–25-fold) the efficiency of recovery of VSV-G in prebudding complexes (Aridor et al., 1998). Identical results were observed when cytosol was used instead of purified COPII components (not shown).

When Sar1 tubules were incubated in the presence of Sec23/24, and Sec13/31 COPII components were imaged using immunoelectron microscopy, we could readily detect Sar1-coated vesicles (Fig. 7 C, a), Sec23-coated vesicles (b), vesicle clusters (c), and vesicular-tubular elements similar to VTCs that contain VSV-G (d). The beads-on-a-string–like appearance of vesicles forming in the presence of Sec23/24 and Sec13/31 are similar to vesicle clusters containing VSV-G that we have previously observed in vivo and in vitro in single-stage complete reactions that contain Sar1-GTP (Aridor et al., 1995; Bannykh et al., 1996) that function as the mobile tubular elements that deliver cargo from the ER to the Golgi in vivo (Presley et al., 1997).

Sequential Recruitment of Sar1 and COPII Leads to Tubule Formation, Export and Delivery of Cargo to the Golgi

Using a well-established cell-free assay (Rowe et al., 1996), we analyzed the role of Sar1 in priming ER export before coat assembly. Microsomes were incubated in a two-stage assay in the presence or absence of Sar1 and COPII components, and the mobilization of VSV-G into the COPII vesicle-containing fraction was analyzed (Fig. 8 A). Preincubation of VSV-G-containing microsomes with Sar1-GTP in stage 1 abolished the requirement for Sar1 in the second stage (Fig. 8 A, b, compare top with bottom). Moreover, the formation of VSV-G-containing COPII vesicles by sequential incubation with Sar1 in stage 1 followed by addition of the Sec23/24 and Sec13/31 complexes in stage 2 occurred as efficiently as when a single incubation was performed in the presence of all three COPII components (Fig. 8 A, d, compare top with bottom). Interestingly, preincubation with Sar1-GTP prevented inhibition of ER export by the dominant–negative Sar1-GDP in

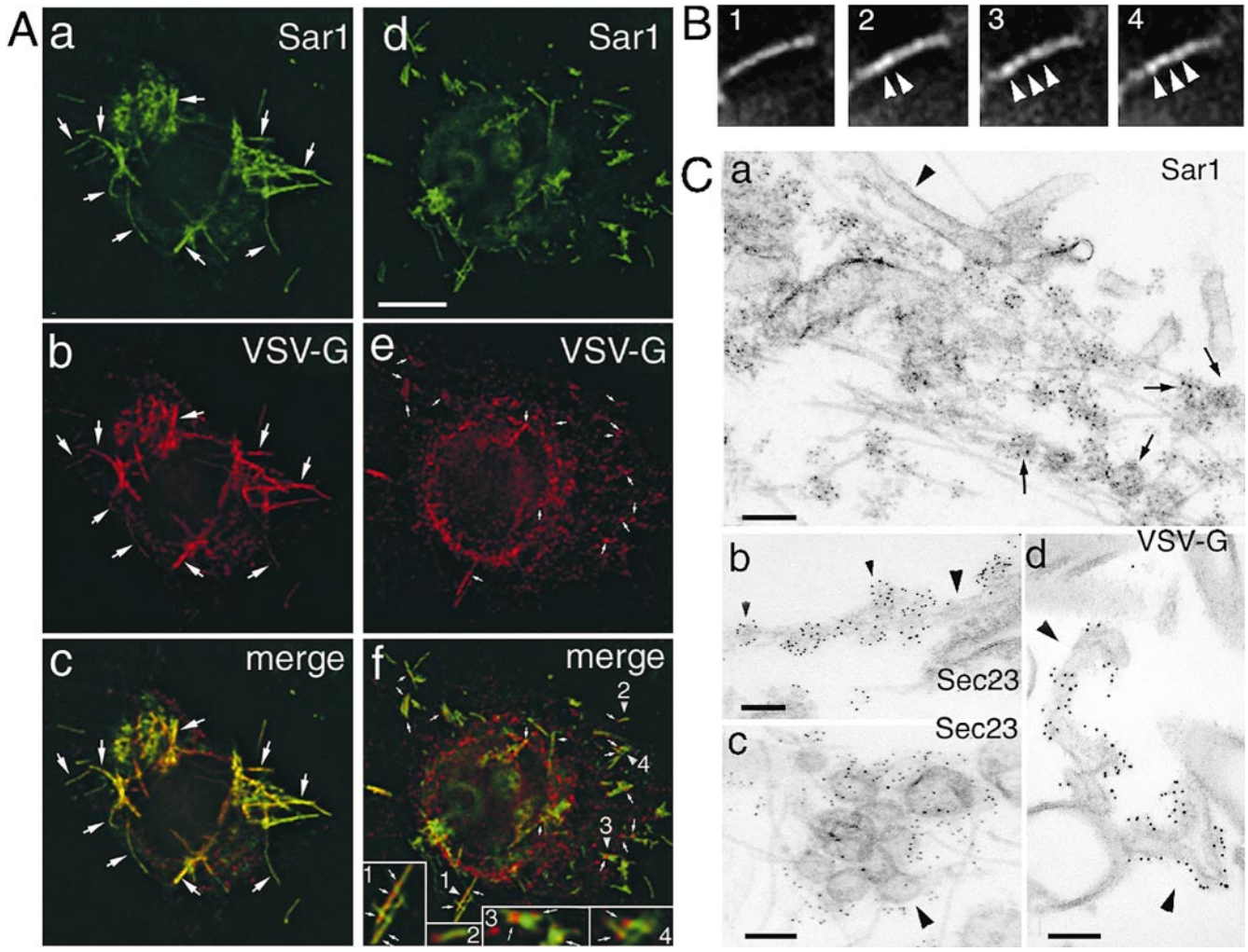

Figure 7. Sar1 tubules are consumed by COPII vesicle budding. (A) Permeabilized NRK cells were incubated for 30 min in the presence of Sar1-GTP to form VSV-G-containing tubules (a–c). Subsequently, the incubation cocktail was replaced with a cocktail containing purified Sec23/24 and Sec13/31 (Aridor et al., 1998) and incubated for an additional 10 min at 32°C (d–f). Cells were labeled for Sar1 (a and d) or VSV-G (b and e) and imaged using a deconvolution microscope. c and f are a merge of a and b, and d and e, respectively. Large arrows in a–c illustrate the overlap of Sar1 with VSV-G. Small arrows in e and f denote location of VSV-G-containing VTCs. Arrowheads in f highlight selected regions (1–4) that demonstrate the appearance of VSV-G-containing punctate VTCs during disassembly of Sar1-containing tubules. The deconvolved image depicts three consecutive 0.1-μm sections (out of 25 total sections) from the middle of the cell to illustrate overlap. Bar in d, 5 μm. (B, 1–4) Time-lapse video (5-min intervals) showing dissolution of Sar1-dependent tubules to form punctate, pre-Golgi–like intermediates containing VSV-G (arrowheads). (C) Permeabilized cells incubated as described above were fixed and processed for electron microscopy as described in Materials and Methods. In a, numerous vesicles (arrows) coated with Sar1 (gold labeled) derived from a region dense in tubules (large arrowhead). (b) Vesicles on tubules and (c) VTCs are shown to contain Sec23. In d, VTCs are shown to contain VSV-G. Bars, 100 nm.

the second stage (Fig. 8 A, c, compare top with bottom). Thus, the initial activation and assembly of Sar1 domains can be temporally separated from the subsequent assembly of remaining COPII coat constituents, as observed morphologically.

To demonstrate that the addition of cytosol to Sar1-GTP–dependent tubules reconstituted normal ER to Golgi traffic, we followed the delivery of VSV-G to the medial Golgi compartment containing the marker Protein A–Man II using indirect immunofluorescence. As shown in Fig. 8 B, incubation in the presence of wild-type Sar1 and GTP resulted in the mobilization of VSV-G to tubular elements that did not overlap with the distribution of Man II (Fig. 8 B, 1). Addition of cytosol led to redistribution of VSV-G to Man II containing Golgi compartments and VTCs (Fig. 8 B, 2). To quantify this result, we followed the ability of VSV-G to be processed to the endoglycosidase H-resistant forms biochemically, a hallmark for processing by cis/medial Golgi enzymes (Davidson and Balch, 1993). Permeabilized cells were pulsed with [^{35}S]-methionine to metabolically label VSV-G, and chased in the presence of Sar1 and GTP to accumulate VSV-G in tubules (stage 1). After addition of cytosol (stage 2), we observed that 30% of total VSV-G was converted to the endo H-resistant form (Fig. 8 B, b), similar to control levels preincubated in the absence of Sar1 (Fig. 8 B, c). Thus, movement of

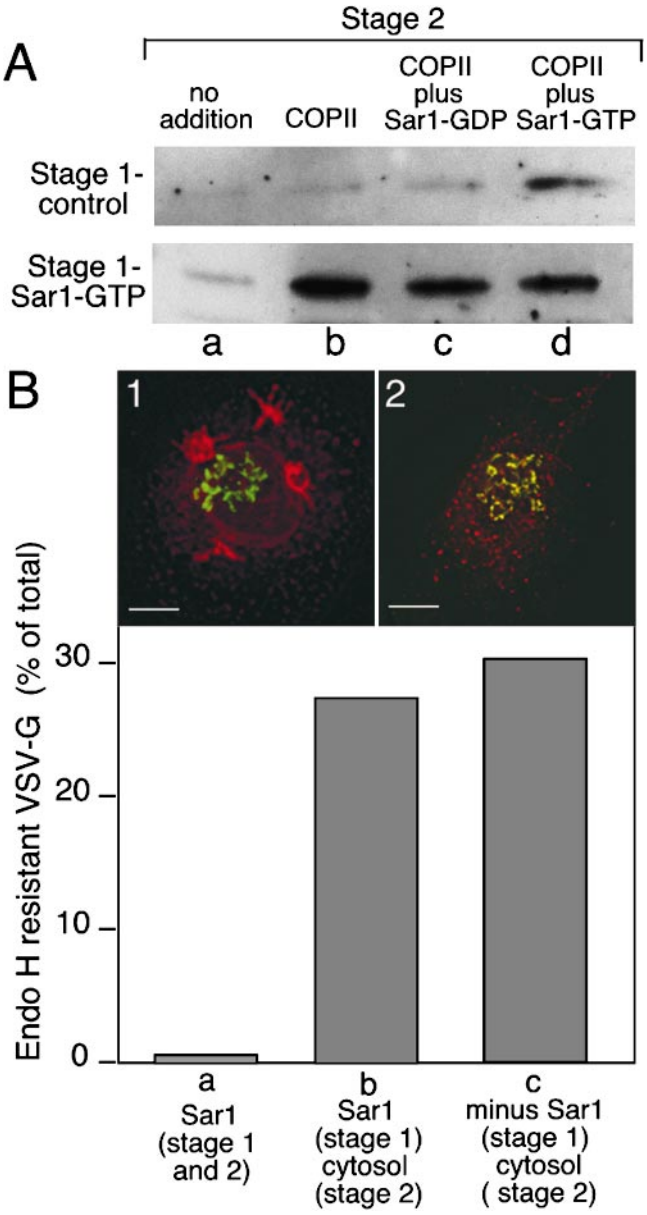

Figure 8. Sar1 tubules are functional intermediates in ER-to-Golgi transport. (A) Microsome membranes containing VSV-G were incubated in the presence (stage 1: Sar1-GTP, bottom) or absence (stage 1: control, top) of Sar1-GTP for 30 min at 32°C. Membranes were collected by centrifugation, washed, and further incubated for additional 30 min at 32°C (stage 2) in the absence (a–c) or presence (d) of Sar1-GTP, in the presence of Sar1-GDP (c), and in the absence (a) or presence (b–d) of purified COPII components Sec23/24 and Sec13/31 (COPII). The fraction containing COPII-coated vesicles was prepared as described (Rowe et al., 1996), and the level of VSV-G recovered determined by immunoblotting with specific antibody (shown). (B) Permeabilized cells were also pulse labeled with [^{35}S]-methionine as described (Davidson and Balch, 1993) and chased for 30 min at 32°C in the presence of wild-type Sar1 and GTP (stage 1) (a). In b, cells were subsequently incubated for 90 min at 32°C in the presence of cytosol. In c, Sar1 and GTP were not included in stage 1 before incubation in the presence of cytosol for 90 min at 32°C. Fractions of VSV-G processed to endo H–resistant forms were reported as a percentage of total VSV-G. (1 and 2) Permeabilized cells were washed and incubated in the presence of wild-type Sar1 and GTP (Stage 1) for 30 min at 32°C. Note the presence of VSV-G in Sar1-dependent tubules (1, rhodamine), but its absence in Man II containing Golgi compartments (1, fluorescein). After Stage 1, cells were further incubated in Stage 2 in the presence of cytosol for 30 min at 32°C. VSV-G shows both punctate localization to VTCs and overlap with Man II-containing compartments (inset 2). Scale bars in 1 and 2: 5 μm.

VSV-G into Sar1-dependent tubules facilitated further mobilization of the cargo molecule to the Golgi complex. Collectively, these results demonstrate that Sar1-GTP tubules are transient and functional intermediates in COPII-mediated export from the ER.

Domain Formation and Cargo Mobilization from the ER In Vivo

The above results suggest that a primary step in ER export in vivo could be tubule formation promoted by the activity of activated Sar1. If this step is rate limiting relative to Sec23/24 recruitment, it should be possible to directly visualize elongated tubular intermediates before vesicle budding.

To focus on the dynamics of ER export site formation in vivo, we used time-lapse fluorescence video microscopy in live cells expressing tsO45 VSV-G tagged with GFP-VSV-G (Fig. 9 mA) (Presley et al., 1997). As shown in sequential images, Fig. 9 B (1–4) (and Movie 2 in the supplemental material), shift of cells from the restrictive (39.5°C) to permissive (32°C) temperature resulted in the redistribution of GFP-VSVG from its diffuse ER distribution into specific export sites readily identifiable by an increase in fluorescence. Often, these cargo-containing ER membranes formed dynamic, elongated tubules that appeared still attached to the reticular membranes of the ER (Fig. 9, B, 1–4, and C, 1–6). Tubules of up to 14 μm (Fig. 9 C, 6) can be readily observed extending from the ER in a process that depends on the integrity of MTs (not shown) (Presley et al., 1997). Once detached, these tubular elements were motile within the cell and moved toward the Golgi complex (not shown, but see Presley et al., 1997). These results suggest that COPII-mediated cargo selection and ER export initiated by the recruitment of Sar1, observed in vitro, can also lead to the formation of selective tubular domains on the ER that collect cargo before export in vivo. These tubular elements may reflect limiting conditions for formation and/or completion of COPII vesicle budding, and therefore serve as important intermediates or transport containers for delivery of cargo to the Golgi complex under the physiological conditions found in living cells.

Discussion

The current study reveals a striking and unanticipated coupling between molecular mechanisms involved in Sar1 activation, biosynthetic cargo selection, and the morphogenesis of ER export sites. We have shown that Sar1 can interact directly with biosynthetic cargo to initiate its mobilization into specialized domains in the ER, independently of COPII coat assembly. By controlling the progress of ER export in vitro, segregation of cargo into specific domains before export is clearly visualized. Incubation of permeabilized cells in the presence of Sar1 alone

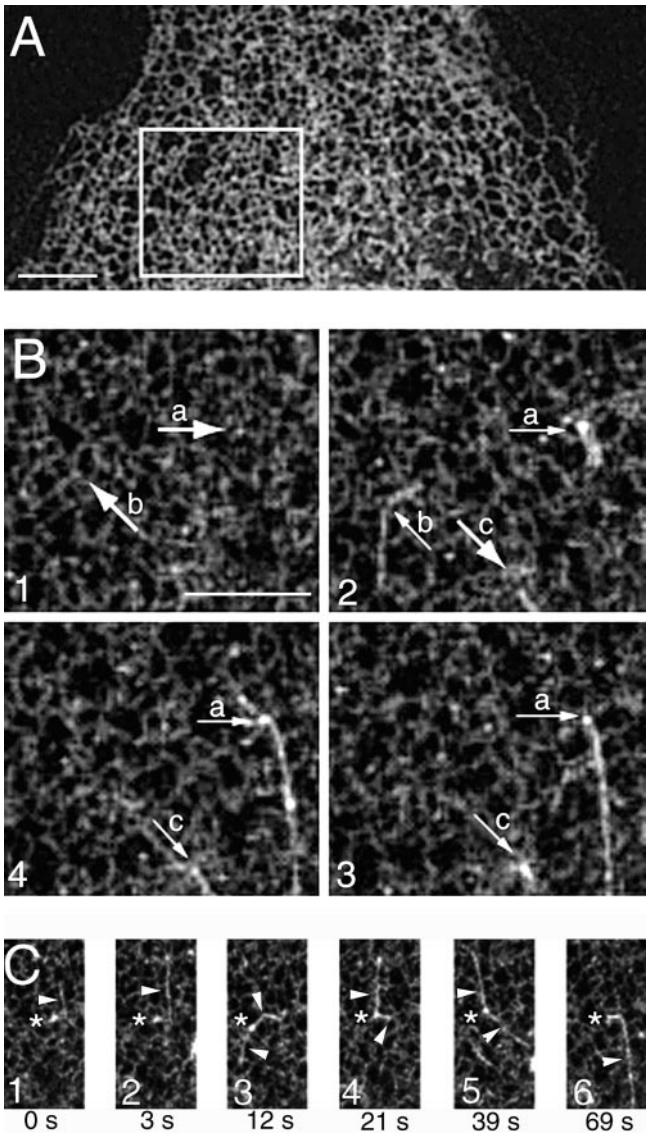

Figure 9. Export of GFP-VSV-G from the ER in living cells. (A) GFP-VSVG expressing COS cells were incubated at 40°C for 12 h to accumulate VSV-G in the reticular ER (A), and then shifted to 32°C to initiate ER export (B). Fluorescence images were taken using time-lapse video microscopy as described in Materials and Methods, and export sites of VSV-G were identified by the increased GFP fluorescence. Scale bar: 5 μm. (B) The boxed area in A is enlarged 2× and the image series (B, 1–4) (1/12-s intervals) is showing the initiation (B1, arrows a and b), formation, and elongation of tubular elements that accumulate and export VSV-G (B, arrows a in 2–4 and c in 3 and 4) from the ER. (C) A detailed time course of tubular elements containing VSV-G repeatedly initiated from the same ER export site at the indicated time points. After detachment, the tubular elements are transported on MTs and are delivered to the Golgi region (not shown) (Presley et al., 1997). In C, 6, the tubule is 14 μm in length. For full video sequence, see Movie 2 in the supplemental material.

led to the formation of ER-derived, cargo-enriched tubular domains, which we believe represent an early intermediate in export from the ER. The highly elongated tubules generated when components essential to promote completion of vesicle budding are withheld are likely to be exaggerated structures formed as a result of the artificially prolonged life time of an otherwise transient intermediate. Several lines of evidence support our hypothesis that these structures are relevant functional intermediates for events occurring in living cells. First, ER tubule formation is blocked by incubation with the dominant–negative Sar1-GDP, attesting to the specificity of the morphological change as an activated Sar1-dependent event that is observed in vivo (Kuge et al., 1994). Second, the elongated tubular elements are reminiscent of the shorter tubular transitional elements that extend from the ER in specialized secretory cells such as pancreatic acinar cells (Palade, 1975), and of ER export complexes found in cells grown in culture (Bannykh et al., 1996). Third, the number of initiation sites for Sar1-dependent tubule formation based on the number of tubules generated in vitro is in full agreement with the typical number of export complexes identified by quantitative morphometry in vivo and in vitro (Saraste and Svensson, 1991; Bannykh et al., 1996; Aridor et al., 1999). Fourth, addition of the remaining COPII constituents to Sar1-generated tubules results in rapid and efficient consumption of these tubules to form VTCs that effectively transport VSV-G to the Golgi. While it is possible that VSV-G could facilitate domain formation in response to release of a bolus of cargo from the ER after temperature shift (Aridor et al., 1999), we do not believe this to generally be the case in that elongated tubules are readily observed in noninfected cells. Fifth, physiological studies in living cells showed that elongated tubular domains can be readily observed when cargo export from the ER is followed dynamically in living cells. Therefore, we propose that Sar1-dependent transitional tubule formation represents an early step in sequential events mediating selective ER export. While our data do not prove that tubule intermediates are the only form of membrane transport between the ER and Golgi in vivo, further studies using live cell microscopy and "live" electron microscopy techniques (Mironov et al., 2000) should provide a means to further address this issue.

Sorting Signals Regulate Coat Assembly

Given the dynamic flow of cargo through the secretory pathway, the regulation of cargo–coat interactions by small GTPases could provide a mechanism to restrict coat assembly and vesicle formation to sites where the GTPase is activated. Our data suggests that sorting signals such as the YxDxE motif involved in ER export (Nishimura and Balch, 1997; Nishimura et al., 1999; Sevier et al., 2000) are not completely effective until a ternary complex containing the sorting signal, the activated GTPase, and the coat is formed (see also Aridor et al., 1998). In general, these biochemical interactions will ensure that the coat only interacts with a subset of cargo molecules present in its target compartment as we report here for Sar1-mediated Sec23/24 interaction with the VSV-G export signals (see also Aridor et al., 1998), or as reported by others for interactions between yeast COPII complexes and SNARE components where ER export signals have yet be identified (Springer and Schekman, 1998).

Tubules Selectively Accumulate Cargo through the Activity of the Sar1 GTPase

Tubules formed in the presence of Sar1 alone begin to accumulate and sort cargo (i.e., VSV-G and Sec22) from ER resident proteins such as BIP and p63 for ER export based

on the qualitative increases in intensity of immunofluorescence, even while connections to the bulk of the ER are clearly evident. These morphological results support previous biochemical observations that detergent-soluble prebudding protein complexes containing cargo and Sar1, or Sar1 and Sec23/24, can be detected before vesicle formation in mammalian cells and yeast (Aridor et al., 1998; Kuehn et al., 1998). Recruitment of the COPII Sec23/24 complex involves coat–cargo interactions that appear to further biochemically stabilize the cargo selection event for export (Aridor et al., 1998). Consistent with these observations, we observed further enrichment of VSV-G based on the increase in fluorescence in punctate intermediates forming on Sar1 tubules in response to the addition of the COPII coat complex Sec23/24. Although the mechanism remains to be established, based on our biochemical results, we suggest that this enhancement of cargo capture is likely to be directed by ternary complexes formed between ER exit codes found on cargo such as VSV-G, activated Sar1, and Sec23/24. Thus, modular components of the COPII coat appear to function in a sequential manner such that Sar1 primes cargo selection events and begins to assemble morphologically distinct export domains in the ER, followed by the recruitment of Sec23/24 to promote efficient capture of cargo into cargo accumulating prebudding complexes. Under physiological conditions, these two stages of cargo capture are tightly coupled and are likely to be occurring within short tubular domains, previously visualized as transitional elements (Palade, 1975). Functional interactions between recruited COPII coat subunits and cargo have also been demonstrated during the export of plasma membrane ATPase, Gas1p, or Sed5p from the ER in vivo in yeast. In each of these cases, dedicated Sec24 subunits, Lst1p or Sfb2p, selectively modulate the efficient capture of the respective cargo protein into the COPII-budding vesicles (Roberg et al., 1999; Peng et al., 2000).

Role of Sar1-dependent Coupling to Microtubules in ER to Golgi Transport

Our results show the morphological appearance of microtubule-assisted tubular export domains following Sar1 activation, suggesting a new level of molecular complexity to ER export. We have provided direct evidence that in addition to the role of Sar1 in directing COPII coat recruitment and assembly, it mediates the recruitment of the microtubule motor kinesin to ER export sites under physiological budding conditions, a result consistent with the prominent distribution of kinesin to pre-Golgi intermediates in vivo (Cole and Lippincott-Schwartz, 1995). These results suggest that COPII vesicle assembly can be coupled with microtubule-dependent transport processes that play a role in either positioning or supporting the elongation of export intermediates, a condition that we have visualized in an exaggerated state by incubating in the absence of additional COPII components. Similar roles for kinesin and microtubules have been suggested for formation or maintenance of the tubular elements comprising ER network (Dabora and Sheetz, 1988; Dreier and Rapoport, 2000). While our results that VTCs can form in vitro after depolymerization of microtubules with nocodazole raises a conundrum regarding their role in Sar1-dependent tubular intermediate formation, a possible resolution to this concern is that depolymerizing reagents do not effect complete disassembly of MTs. Short microtubule elements that cannot be depolymerized may mediate the local VTC formation in vitro. Further work is required to demonstrate a direct coupling between tubule formation and MTs for ER export in vivo. The potential role of microtubules in tubule formation is further supported by the observation that yeast Sar1 interacts with MTs (Barnes et al., 1992). Moreover, 50–60% of ER export sites as analyzed by quantitative EM are actively positioned at the perinuclear region close to the microtubule organizing center (Bannykh et al., 1996).

The difficulty in detecting microtubule-dependent processes in ER-to-Golgi transport in vivo is further exemplified by the fact that transport of cargo has frequently been reported to be insensitive to disruption of microtubules by exposure to MT-depolymerizing agents. However, both electron and video microscopy now strongly support the role of MTs in the transport of pre-Golgi intermediates from their site of formation at peripheral ER exit sites to the central Golgi region using the molecular motor dynein (Saraste and Svensson, 1991; Presley et al., 1997). Moreover, during the time period preceding Golgi dispersal from its central location to peripheral ER export sites in response to MT depolymerization, transport of GFP-VSV-G localized to pre-Golgi intermediates has been shown to be inhibited (Presley et al., 1997). Our results now emphasize the possible involvement of Sar1 in coordinating even earlier microtubule-dependent events associated with COPII–mediated cargo selection (Barlowe et al., 1994, Aridor et al., 1998) and kinesin-mediated events. Thus, microtubule-dependent vectorial processes are likely to help direct traffic from the ER to the Golgi in vivo.

Higher Order Molecular Interactions May Facilitate ER Export Site Selection

The ability of Sar1 to form intermediate tubular domains that participate in selective ER export and transport to the Golgi suggests that the molecular mechanism(s) involved in tubular intermediate formation can be an integral part of the COPII budding step. Indeed, the ability to stabilize tubular intermediates by omitting COPII components suggests that the transition between tubules and vesicles is tightly regulated by sequential coat recruitment in response to the GTPase activity. Thus, differences in the morphology of ER export sites in different cells may reflect the differential steady state regulation of a sequential COPII assembly process that is required to adapt the rates of ER export with either the needs of the cell for packaging a biologically diverse range of cargo species (Aridor and Balch, 1999) or to be compatible with the morphological organization of its secretory pathway. One possibility is that the levels of individual COPII components in different cells (reflected in their abundance at ER export sites) may play an important role in the balance of vesicles or tubule intermediates formed. Alternatively, posttranslational modifications may regulate the vesicle/tubule balance (Aridor and Balch, 2000). The ability to modulate tubule/vesicle formation may also provide a facile mechanism to accommodate the transport of bulky cargo that exceeds the restricted size of typical vesicular carriers (50–80 nm). For example, procollagen (200 nm in length) may leave the ER preferentially in Sar1-induced tubular elements (Bonfanti et al., 1998). This is consistent with our recent obser-

vations that cargo can modulate the activity of the COPII vesicle budding machinery, supporting the proposal that cargo can regulate ER export (Aridor et al., 1999).

The use of tubular transport intermediates in different sorting sites in the exocytic and endocytic pathways in vivo has been well documented. Transient, tubular transport intermediates have been observed for export from the TGN (Hirschberg et al., 1998; Toomre et al., 1998). Tubules are formed within the Golgi complex and are involved in retrograde transport to the ER (Sciaky et al., 1997). Finally, tubules are observed during transport between endosomal compartments (Aniento et al., 1993; Hopkins et al., 1994; Faigle et al., 1998). Our results would therefore suggest that different coat complexes that are involved in vesicle formation at these various sorting sites may also use tubular intermediates to achieve sorting and transport.

In conclusion, we have provided a molecular link between the dynamic morphology of ER export site formation and the biochemical machinery used for cargo selection. We propose that the interactions reported here between cargo and Sar1 define a primary level of cargo selection that initiates coat assembly and prebudding complex formation (Aridor et al., 1998; Kuehn et al., 1998) to direct protein sorting. This is a property shared by other coat complexes in the secretory and endocytic pathway that can be reconstituted using artificial systems (Matsuoka et al., 1998; Spang et al., 1998; Takei et al., 1998; Bremser et al., 1999). We suggest that this primary level of cargo recruitment and sorting is integrated with a second level of morphological organization that couples export domain formation with cargo selection through activation of the Sar1 GTPase. We propose that this coupling can modulate the regional organization of the ER to improve the fidelity and efficiency of the sorting process.

This work was supported by a grant to W.E. Balch from the National Institutes of Health (GM42336) and involved extensive use of Cores B and C in CA58689. K.N. Fish is a recipient of the Helen L. Dorris Research Award.

Submitted: 24 July 2000
Revised: 1 November 2000
Accepted: 3 November 2000

References

Allan, B.B., and W.E. Balch. 1999. Protein sorting by directed maturation of Golgi compartments. *Science*. 285:63–66.

Allan, B.B., B.D. Moyer, and W.E. Balch. 2000. Rab1 recruitment of p115 into a cis-SNARE complex: programming budding COPII vesicles for fusion. *Science*. 289:444–448.

Allan, V., and R. Vale. 1994. Movement of membrane tubules along microtubules in vitro: evidence for specialised sites of motor attachment. *J. Cell Sci*. 107:1885–1897.

Aniento, F., N. Emans, G. Griffiths, and J. Gruenberg. 1993. Cytoplasmic dynein-dependent vesicular transport from early to late endosomes. *J. Cell Biol.* 123:1373–1387.

Aridor, M., and W.E. Balch. 1996. Principles of selective transport: coat complexes hold the key. *Trends Cell Biol.* 6:315–320.

Aridor, M., and W.E. Balch. 1999. Integration of endoplasmic reticulum signaling in health and disease. *Nat. Med.* 5:745–751.

Aridor, M., and W.E. Balch. 2000. Kinase signaling initiates COPII recruitment and export from the mammalian endoplasmic reticulum. *J. Biol. Chem.* 275: 35673–35676.

Aridor, M., S.I. Bannykh, T. Rowe, and W.E. Balch. 1995. Sequential coupling between COPII and COPI vesicle coats in endoplasmic reticulum to Golgi transport. *J. Cell Biol.* 131:875–893.

Aridor, M., S.I. Bannykh, T. Rowe, and W.E. Balch. 1999. Cargo can modulate the formation of COPII coated vesicles. *J. Biol. Chem.* 274:4389–4399.

Aridor, M., J. Weissman, S. Bannykh, C. Nuoffer, and W.E. Balch. 1998. Cargo selection by the COPII budding machinery during export from the endoplasmic reticulum. *J. Cell Biol.* 141:61–70.

Balch, W.E., J.M. McCaffery, H. Plutner, and M.G. Farquhar. 1994. Vesicular stomatitis virus glycoprotein is sorted and concentrated during export from the endoplasmic reticulum. *Cell*. 76:841–852.

Bannykh, S., N. Nishimura, and W.E. Balch. 1998. Getting into the Golgi. *Trends Cell Biol.* 8:21–25.

Bannykh, S.I., T. Rowe, and W.E. Balch. 1996. Organization of endoplasmic reticulum export complexes. *J. Cell Biol.* 135:19–35.

Barlowe, C., L. Orci, T. Yeung, M. Hosobuchi, S. Hamamoto, N. Salama, M.F. Rexach, M. Ravazzola, M. Amherdt, and R. Schekman. 1994. COPII: a membrane coat formed by Sec proteins that drive vesicle budding from the endoplasmic reticulum. *Cell*. 77:895–907.

Barnes, G., K.A. Louie, and D. Botstein. 1992. Yeast proteins associated with microtubules in vitro and in vivo. *Mol. Biol. Cell*. 3:29–47.

Bonfanti, L., A.A. Mironov, Jr., J.A. Martinez-Menarguez, O. Martella, A. Fusella, M. Baldassarre, R. Buccione, H.J. Geuze, A.A. Mironov, and A. Luini. 1998. Procollagen traverses the Golgi stack without leaving the lumen of cisternae: evidence for cisternal maturation. *Cell*. 95:993–1003.

Bremser, M., W. Nickel, M. Schweikert, M. Ravazzola, M. Amherdt, C.A. Hughes, T.H. Sollner, J.E. Rothman, and F.T. Wieland. 1999. Coupling of coat assembly and vesicle budding to packaging of putative cargo receptors. *Cell*. 96:495–506.

Cole, N.B., and J. Lippincott-Schwartz. 1995. Organization of organelles and membrane traffic by microtubules. *Curr. Opin. Cell Biol.* 7:55–64.

Cosson, P., and F. Letourneur. 1997. Coatomer (COPI)-coated vesicles: role in intracellular transport and protein sorting. *Curr. Opin. Cell Biol.* 9:484–487.

Dabora, S.L., and M.P. Sheetz. 1988. The microtubule-dependent formation of a tubulovesicular network with characteristics of the ER from cultured cell extracts. *Cell*. 54:27–35.

Davidson, H.W., and W.E. Balch. 1993. Differential inhibition of multiple vesicular transport steps between the endoplasmic reticulum and trans Golgi network. *J. Biol. Chem.* 268:4216–4226.

Dreier, L., and T.A. Rapoport. 2000. In vitro formation of the endoplasmic reticulum occurs independently of microtubules by a controlled fusion reaction. *J. Cell Biol.* 148:883–898.

Faigle, W., G. Raposo, D. Tenza, V. Pinet, A.B. Vogt, H. Kropshofer, A. Fischer, G. de Saint-Basile, and S. Amigorena. 1998. Deficient peptide loading and MHC class II endosomal sorting in a human genetic immunodeficiency disease: the Chediak-Higashi syndrome. *J. Cell Biol*. 141:1121–1134.

Heuser, J.E., and J. Keen. 1988. Deep-etch visualization of proteins involved in clathrin assembly. *J. Cell Biol.* 107:877–886.

Hirschberg, K., C.M. Miller, J. Ellenberg, J.F. Presley, E.D. Siggia, R.D. Phair, and J. Lippincott-Schwartz. 1998. Kinetic analysis of secretory protein traffic and characterization of Golgi to plasma membrane transport intermediates in living cells. *J. Cell Biol.* 143:1485–1503.

Hopkins, C.R., A. Gibson, M. Shipman, D.K. Strickland, and I.S. Trowbridge. 1994. In migrating fibroblasts, recycling receptors are concentrated in narrow tubules in the pericentriolar area, and then routed to the plasma membrane of the leading lamella. *J. Cell Biol.* 125:1265–1274.

Kuehn, M.J., J.M. Herrmann, and R. Schekman. 1998. COPII-cargo interactions direct protein sorting into ER-derived transport vesicles. *Nature*. 391: 187–190.

Kuge, O., C. Dascher, L. Orci, T. Rowe, M. Amherdt, H. Plutner, M. Ravazzola, G. Tanigawa, J.E. Rothman, and W.E. Balch. 1994. Sar1 promotes vesicle budding from the endoplasmic reticulum but not Golgi compartments. *J. Cell Biol.* 125:51–65.

Lane, J.D., and V.J. Allan. 1999. Microtubule-based endoplasmic reticulum motility in *Xenopus laevis*: activation of membrane-associated kinesin during development. *Mol. Biol. Cell*. 10:1909–1922.

Martinez-Menarguez, J.A., H.J. Geuze, J.W. Slot, and J. Klumperman. 1999. Vesicular tubular clusters between the ER and Golgi mediate concentration of soluble secretory proteins by exclusion from COPI-coated vesicles. *Cell*. 98:81–90.

Matsuoka, K., L. Orci, M. Amherdt, S.Y. Bednarek, S. Hamamoto, R. Schekman, and T. Yeung. 1998. COPII-coated vesicle formation reconstituted with purified coat proteins and chemically defined liposomes. *Cell*. 93:263–275.

Mironov, A.A., R.S. Polishchuk, and A. Luini. 2000. Visualizing membrane traffic in vivo by combined video fluorescence and 3D electron microscopy. *Trends Cell Biol*. 10:349–353.

Nishimura, I., T. Uetsuki, S.U. Dani, Y. Ohsawa, I. Saito, H. Okamura, Y. Uchiyama, and K. Yoshikawa. 1998. Degeneration in vivo of rat hippocampal neurons by wild-type Alzheimer amyloid precursor protein overexpressed by adenovirus-mediated gene transfer. *J. Neurosci.* 18:2387–2398.

Nishimura, N., and W.E. Balch. 1997. A di-acidic signal required for selective export from the endoplasmic reticulum. *Science*. 277:556–558.

Nishimura, N., S. Bannykh, S. Slabough, J. Matteson, Y. Altschuler, K. Hahn, and W.E. Balch. 1999. A di-acidic (DXE) code directs concentration of cargo during export from the endoplasmic reticulum. *J. Biol. Chem.* 274: 15937–15946.

Palade, G.E. 1975. Intracellular aspects of the process of protein transport. *Science*. 189:347–354.

Peng, R., A. De Antoni, and D. Gallwitz. 2000. Evidence for overlapping and

distinct functions in protein transport of coat protein Sec24p family members. *J. Biol. Chem*. 275:11521–11528.

Plutner, H., H.W. Davidson, J. Saraste, and W.E. Balch. 1992. Morphological analysis of protein transport from the endoplasmic reticulum to Golgi membranes in digitonin permeabilized cells: role of the p58 containing compartment. *J. Cell Biol.* 119:1097–1116.

Presley, J.F., N.B. Cole, T.A. Schroer, K. Hirschberg, K.J.M. Zaal, and J. Lippincott-Schwartz. 1997. ER-to-Golgi transport visualized in living cells. *Nature*. 389:81–84.

Rexach, M.F., M. Latterich, and R.W. Schekman. 1994. Characteristics of endoplasmic reticulum-derived transport vesicles. *J. Cell Biol.* 126:1133–1148.

Roberg, K.J., M. Crotwell, P. Espenshade, R. Gimeno, and C.A. Kaiser. 1999. *LST1* is a *SEC24* homologue used for selective export of the plasma membrane ATPase from the endoplasmic reticulum. *J. Cell Biol.* 145:659–672.

Rowe, T., M. Aridor, J.M. McCaffery, H. Plutner, and W.E. Balch. 1996. COPII vesicles derived from mammalian endoplasmic reticulum (ER) microsomes recruit COPI. *J. Cell Biol.* 135:895–911.

Rowe, T., and W.E. Balch. 1995. Expression and purification of mammalian Sar1. *Methods Enzymol.* 257:49–53.

Rowe, T., C. Dascher, S. Bannykh, H. Plutner, and W.E. Balch. 1998. Role of vesicle-associated syntaxin 5 in the assembly of pre-Golgi intermediates. *Science*. 279:696–700.

Saraste, J., and K. Svensson. 1991. Distribution of the intermediate elements operating in ER to Golgi transport. *J. Cell Sci.* 100:415–430.

Scales, S.J., R. Pepperkok, and T.E. Kreis. 1997. Visualization of ER-to-Golgi transport in living cells reveals a sequential mode of action for COPII and COPI. *Cell*. 90:1137–1148.

Schwaninger, R., C.J.M. Beckers, and W.E. Balch. 1991. Sequential transport of protein between the endoplasmic reticulum and successive Golgi compartments in semi-intact cells. *J. Biol. Chem.* 266:13055–13063.

Sciaky, N., J. Presley, C. Smith, K.J. Zaal, N. Cole, J.E. Moreira, M. Terasaki, E. Siggia, and J. Lippincott-Schwartz. 1997. Golgi tubule traffic and the effects of brefeldin A visualized in living cells. *J. Cell Biol*. 139:1137–1155.

Sevier, C.S., O.A. Weisz, M. Davis, and C.E. Machamer. 2000. Efficient export of the vesicular stomatitis virus G protein from the endoplasmic reticulum requires a signal in the cytoplasmic tail that includes both tyrosine-based and di-acidic motifs. *Mol. Biol. Cell*. 11:13–22.

Spang, A., K. Matsuoka, S. Hamamoto, R. Schekman, and L. Orci. 1998. Coatomer, Arf1p, and nucleotide are required to bud coat protein complex I-coated vesicles from large synthetic liposomes. *Proc. Natl. Acad. Sci. USA*. 95:11199–11204.

Springer, S., and R. Schekman. 1998. Nucleation of COPII vesicular coat complex by endoplasmic reticulum to Golgi vesicle SNAREs. *Science*. 281:698–700.

Storrie, B., R. Pepperkok, E.H. Stelzer, and T.E. Kreis. 1994. The intracellular mobility of a viral membrane glycoprotein measured by confocal microscope fluorescence recovery after photobleaching. *J. Cell Sci.* 107:1309–1319.

Takei, K., V. Haucke, V. Slepnev, K. Farsad, M. Salazar, H. Chen, and P. De Camilli. 1998. Generation of coated intermediates of clathrin-mediated endocytosis on protein-free liposomes. *Cell*. 94:131–141.

Terasaki, M., and T.S. Reese. 1992. Characterization of endoplasmic reticulum by co-localization of BiP and dicarbocyanine dyes. *J. Cell Sci.* 101:315–322.

Toomre, D., P. Keller, J. White, J.C. Olivo, and K. Simons. 1998. Dual-color visualization of trans–Golgi network to plasma membrane traffic along microtubules in living cells. *J. Cell Sci.* 112:21–33.

Velasco, A., L. Hendricks, K.W. Moreman, D.R.P. Tulsiani, O. Touster, and M.G. Farquhar. 1993. Cell type–dependent variations in the subcellular distribution of α-mannosidase I and II. *J. Cell Biol.* 122:39–51.

Weiss, O., J. Holden, C. Rulka, and R.A. Kahn. 1989. Nucleotide binding and cofactor activities of purified bovine brain and bacterially expressed ADP-ribosylation factor. *J. Biol. Chem.* 264:21066–21072.